Tropical Cyclones in the 7km NASA Global Nature Run for use in Observing System Simulation Experiments

Oreste Reale[*] [†], Deepthi Achuthavarier [‡],

Marangelly Fuentes [§], William M. Putman, and Gary Partyka[¶]

Global Modeling and Assimilation Office, NASA, Greenbelt, Maryland, USA

[*]*Corresponding author address:* Oreste Reale, NASA Goddard Space Flight Center, Code 610.8, Greenbelt, MD 20771.

E-mail: oreste.reale-1@nasa.gov

[†]Universities Space Research Association, Goddard Earth Sciences, Technology and Research, Columbia, Maryland, USA

[‡]Universities Space Research Association, Goddard Earth Sciences, Technology and Research, Columbia, Maryland, USA

[§]Science Systems and Applications, Inc., Greenbelt, Maryland, USA

[¶]Science Systems and Applications, Inc., Greenbelt, Maryland, USA

ABSTRACT

The National Aeronautics and Space Administration (NASA) Nature Run (NR), released for use in Observing System Simulation Experiments (OSSEs), is a 2-year long global non-hydrostatic free-running simulation at a horizontal resolution of 7 km, forced by observed sea-surface temperatures (SSTs) and sea ice, and inclusive of interactive aerosols and trace gases. This article evaluates the NR with respect to tropical cyclone (TC) activity. It is emphasized that to serve as a NR, a long-term simulation must be able to produce realistic TCs, which arise out of realistic large-scale forcings. The presence in the NR of the realistic, relevant dynamical features over the African Monsoon region and the tropical Atlantic is confirmed, along with realistic African Easterly Wave activity. The NR Atlantic TC seasons, produced with 2005 and 2006 SSTs, show interannual variability consistent with observations, with much stronger activity in 2005. An investigation of TC activity over all the other basins (eastern and western North Pacific, North and South Indian Ocean, and Australian region), together with relevant elements of the atmospheric circulation, such as, for example, the Somali Jet and westerly bursts, reveals that the model captures the fundamental aspects of TC seasons in every basin, producing realistic number of TCs with realistic tracks, life spans and structures. This confirms that the NASA NR is a very suitable tool for OSSEs targeting TCs and represents an improvement with respect to previous long simulations that have served the global atmospheric OSSE community.

1. Introduction

Observing Systems Experiments (OSEs), also known as ‘data impact studies’, represent a procedure to explore the impact of an *existing* instrument on a given forecasting capability. OSEs require a comprehensive set of observations, a Data Assimilation System (DAS) and a forecast model. At least two sets of parallel analyses are produced by assimilating a) the comprehensive observational data set (ideally comprising all the data operationally used) and b) the same observational set with or without the data from the specific instrument whose impact is being investigated. Corresponding sets of parallel forecasts are initialized from each set of analyses, so that their different skills can be assessed with various metrics against some validating analyses.

In contrast, Observing Systems *Simulation* Experiments (OSSEs) are often used by atmospheric scientists and instrument developers to evaluate the potential impact of a *future* instrument. With respect to OSEs, an OSSE framework requires a ‘Nature Run’ (NR) and a methodology for simulating realistic observations, in addition to the DAS and forecast model. A NR is a free-running simulation produced by a state-of-the-art model, and is supposed to satisfy many stringent requirements, one being ‘a realistic climatology consisting of *realistic weather patterns*’ (McCarty et al. 2012). The NR is needed to extract simulated synthetic observations of a future sensor which are assimilated, together with the simulated observations of the existing sensors, in the DAS, producing sets of analyses from which forecasts can be issued.

One fundamental difference between OSEs and OSSEs is that in OSSEs the ‘true’ atmospheric state is precisely known from the NR. Consequently, instrument errors can be explicitly formulated and OSSEs can be also used to explore analysis error statistics of already existing observing systems (Errico et al. 2007). For a comprehensive review of OSSEs see, among others, Errico et al. (2013), Privé et al. (2013a), Privé et al (2013b), Atlas et al. (2015), Ma et al. (2015), Hoffman and Atlas (2016).

The purpose of this article is to evaluate the realism of the new 7-km National Aeronautics and Space Administration (NASA) NR with respect to tropical cyclone (TC) activity. Two caveats are necessary. First of all, it is important to clarify that different Instrument Science Teams may have different requirements for a NR to be considered realistic. This particular assessment aims at demonstrating that this new NR can: a) produce realistic TCs from realistic large-scale forcings and b) represent features at scales of about 15 km around TCs. As such, the Science Team for Cyclone Global Navigation Satellite System (CYGNSS) or other teams focused on comparable future instruments could benefit from this NR to produce realistic OSSEs focused on the prediction of wind features around high-impact weather systems, such as TCs and intense extratropical disturbances. Teams performing OSSEs for measurements at much higher resolution could still benefit from this NR by using it as a forcing for downscaled simulations, strategy previously documented by Nolan et al. (2013).

Second, the terms ‘evaluation’ and ‘assessment’ are preferred to ‘validation’ in this work. The reason is that a NR cannot strictly be ‘validated’ as an actual forecast can be. In fact, being a free simulation forced by sea surface temperatures (SSTs) and sea ice, weather events in a NR cannot match corresponding actual weather events, since the memory of initial conditions is lost within a few weeks. Time in the NR does not correspond to factual time, except that we may expect some statistical similarity on an interannual basis due to the real SST and sea ice that are used. The evaluation of NR therefore comprises two steps: an overall assessment of its statistical properties, as complete as possible (which is not the subject of this article), and a verification that these statistics arise out of instantaneously ‘meaningful’ states of the atmosphere. A phenomenological approach showcasing comparisons between weather events in the NR and weather events in the real world is one way to investigate instantaneous states of the atmosphere. These comparisons are the focus of this article.

The article is organized as follows: Section 2 discusses TCs as detected in previous NRs; Section 3 provides a general description of the new NASA NR and of the extensive team evaluation effort which has already been carried out; Section 4 focuses on an examination of NR TC activity compared to observations over the various basins (Atlantic, eastern North Pacific, western North Pacific, North Indian and South Indian Oceans, Australian region). Elements of the circulation which are important in TC formation or in controlling the TC evolution are also discussed. Lastly, Section 5 states the conclusions of this work.

2. Tropical Cyclone Activity and Structure in previous Nature Runs

Considering the cost of spaceborne instruments, a realistic estimate of their potential benefit is exceptionally important, hence the ‘political’ and economical implications of OSSEs. However, in order to be realistic and credible, a standardized OSSE framework would be desirable. OSSEs do not provide the desired benefit if different investigators perform them for the same instrument and obtain contrasting results.

An important source of discrepancy in OSSEs can arise out of the use of different NRs. Even if the same NR is used, OSSEs credibility could be hindered by the use of: a) NRs whose quality is not sufficiently good or whose resolution is inadequate; b) NRs whose realism have not been investigated in depth; c) NRs which are too close to the forecast model, potentially resulting in the so-called ‘identical twin problem’ (Atlas 1997).

Ideally, the NR should be as far from the forecast model as the true atmosphere (Hoffman et al., 1990) is. Aside from the difficulty of attaining this goal, the creation of a NR for widespread use is a nontrivial matter. The NR should be among the best possible simulations available at a given time. It should also be evaluated by, distributed to, and shared with, a large OSSE community. To produce a global Nature Run with these requirements is a demanding and extraordinarily computationally expensive task that only few centers in the world can afford. For this, among other reasons, multi-agency collaborations to standardize OSSEs were attempted as early as the mid-80s (e.g., Atlas et al. 1985; Arnold and Dey 1986). With this frame of mind, a renewed international informal collaboration, often referred to as 'Joint OSSE' project, between scientists in different agencies and centers including, but not limited to, the European Center for Medium-Range Weather Forecasts (ECMWF), the National Ocean and Atmosphere Administration (NOAA), NASA, was initiated in the mid 2000s (Masutani et al. 2007; Kleist and Ide 2015). As part of this collaborative effort, the ECMWF produced and released in 2006 a one-year long NR to serve the OSSE community.

The ECMWF NR, hereafter referred to the ECMWF T511 NR, was produced at a T511 wave truncation, corresponding to an actual resolution of about 40 km at the Equator and was documented, among several others, by Reale et al. (2007), Masutani et al. (2010), Andersson and Matusani (2010) and McCarty et al. (2012). Amidst many outstanding and unprecedented qualities, the ECMWF T511 NR was arguably considered the first free-running long simulation, forced by prescribed 2005 SSTs and sea-ice, which produced a realistic depiction of TC activity. The TC activity was considered 'realistic' because: a) the average climatological factors that are conducive to cyclogenesis were present, and b) the frequency, distribution, life cycle, and track of TCs were within observed climatological values. The team evaluation of the ECMWF T511 NR demonstrated not only that TCs were present, but that they originated out of realistic and very specific weather patterns associated with TC genesis in reality. The evaluation also showed that TCs produced by the ECMWF T511 NR underwent realistic evolution and decay, including dissipation, landfall, extra-tropical transitions and binary vortex interaction. Moreover, individual TCs displayed an overall realistic structure in terms of vertical alignment, presence of a warm-core, low-level winds in excess of 50 ms^{-1} and an eye-like feature (i.e., a virtually windless column), as shown by Reale et al. (2007). While the eye-like feature was broader and more diluted than a real TC eye, due to limited T511 horizontal resolution, the ECMWF T511 NR nevertheless represented a remarkable modeling achievement and has been serving as an invaluable tool for several years. Among others, the NOAA Earth System Research Laboratory OSSE capability (Privé et al. 2013c), the NASA Global Modeling and Assimilation Office (GMAO) OSSE baseline (Errico et al. 2013) and framework (Privé et al. 2013b) had been built on the ECMWF T511 NR.

However, since 2006, with the exponential growth in high-end computing resources, the associated increase in global models' resolution, and the steady augmentation of new sensors' capabilities, there are multiple reasons to create a new nature run. NASA has a special interest in OSSEs, because they enable instrument developers to conceive, justify and develop new sensors. Aside from assisting the design of a future sensor, OSSEs are also an essential tool for Science Teams of instruments which are already designed and scheduled to launch, but not in space yet, because OSSEs can be used to design, develop, and test the new data assimilation procedures needed to maximize the lifetime utility of the new sensor. An example, documented by Annane et al. (2015), is focused on the mission CYGNSS, which has an expected launch in October 2016.

Pressed by these needs, a number of long simulations at increasing resolutions have been produced over the years by the GMAO with a similar configuration to the ECMWF T511 NR: initialization in May 2005, prescribed SSTs and sea ice, but with the integration extending more than two years in order to have a measure of some interannual variability. Comprehensive assessments were performed by this and other teams.

From the point of view of TCs, which are the focus of this article, particularly noteworthy was the 2-year cubed-sphere c720 simulation at 14-km horizontal resolution (Putman and Suarez

2011). It represented an important advance, in that it produced not only a reasonable number of TCs, but also a very good representation of the interannual variability in TC activity observed between 2005 and 2006. Additional GMAO two-year simulations with the same settings, but at 10 km resolution, were also produced and provided further improvement (not shown). These long simulations and others were all evaluated as potential next-generation NRs but ended up representing only intermediate steps towards the NR that eventually was publicly released in 2015 by the GMAO, and which is the subject of this investigation.

3. The 7-km NASA Nature Run

a. General description and comprehensive team evaluation

The new NASA NR, produced with a cubed-sphere non-hydrostatic mesoscale version of the Global Earth Observing System, version 5, (GEOS-5) model, is described in great detail in the comprehensive NASA Technical Memorandum (Gelaro et al. 2015), which is a public document available online. The GEOS-5 NR (hereafter referred to as G5NR) was run with a cubed-sphere geometry of 1440×1440 grid cells (c1440) within each of the six faces of the gnomonic cube-sphere grid (Putman and Lin 2007) nearly uniformly distributed around the globe. This corresponds to a horizontal resolution of about 7km around the equator [$40,000\,km/(1440 \times 4$ grid cells)$\approx 7\,km$]. The G5NR is thus capable of partially resolving features as small as mesoscale complexes and TCs.

A major collaborative effort, involving several months of work by a multidisciplinary team of about 25 scientists, was necessary to evaluate the G5NR. As part of this effort, Putman (2015) provides a general overview of the model aspects and an overall description of the type of phenomena that can be represented in the simulation. Privé et al (2015) give a general statistical evaluation of wind and temperature, inclusive of spectral analysis, comparing it with reanalysis data and confirming the overall realism of the NR. Molod et al. (2015) investigate in depth humidity and precipitation fields, comparing the G5NR with both reanalyses and observational data sets. Draper et al. (2015) investigates the surface characteristics from land, ocean and ice perspectives. Norris et al. (2015) performs an evaluation of clouds and radiation in the NR against Clouds and the Earth's Radiant Energy System (CERES) and Cloud-Aerosol Lidar with Orthogonal Polarization (CALIOP) data. Ott et al. (2015) produces an assessment of the representation and realism of aerosol and trace gases in the NR. It should be emphasized that the treatment of radiatively active aerosols and trace gases is a novel feature for the OSSE community, made possible by the inclusion of the Goddard Chemistry, Aerosol, Radiation and Transport Model (GOCART, Chin et al. 2002), which is coupled with the GEOS-5 radiation code (Colarco et al. 2010). From the perspective of TCs, which are the subject of this article, previous work had demonstrated that the impact of interactive treatment of Saharan dust improves the representation of the African Easterly Jet in the GEOS-5 (Reale et al. 2011) and affects tropical cyclogenetic processes (Reale et al. 2014).

Aside from the evaluation of a NR's comprehensive statistical properties, which may differ up to a certain acceptable threshold (within observed natural variability) from the corresponding properties of the real atmosphere, it is important to evaluate any NR from a phenomenological perspective, i.e., focusing on snapshots of specific weather events. While these events cannot correspond to actual events occurred in the real world, they nevertheless must constitute an acceptable representation of something 'possible', falling within the range of observed phenomena.

In fact, OSSEs are often carried out by targeting *one* specific weather event simulated in the NR. Analyses are created by assimilating synthetic observations extracted from NR states preceding that specific event, and forecasts can be initialized from those analyses. Therefore, an OSSE can give information on whether the addition of a new sensor can enhance the ability to ‘predict’ that event, using the NR as a validating ‘truth’.

b. Weather phenomena and possible use of the G5NR

Aside from TCs, which are the subject of this article, it is important to mention that the G5NR has been investigated also from the point of view of other weather phenomena that may be of interest to scientists developing OSSEs.

For example, Putman (2015), discussing resolved features, finds great realism in the overall distribution of extra-tropical cyclone track and genesis location. Of interest for future OSSEs targeting instruments focused on frozen precipitation, is the study of intense baroclinic winter cyclones, such as, for example, US mid-Atlantic snowstorms. In this regard, Putman (2015) showcases an example of a simulated major US east-coast snowstorm whose track and accumulated precipitation bear a remarkable similarity with observational records (e.g., Kocin and Uccellini 2005).

Another example of a well-reproduced phenomena are several cases of Extra-Tropical Transitions (ETs). During ET, a warm-cored cyclone evolves into a larger scale baroclinic system through a number of transformations that include, among others, a change in its primary energy source from latent heat to baroclinic energy conversion processes (e.g, Sinclair 1993; Kyle and Bosart 2014). A very representative case is highlighted in the comprehensive NASA Tech Memo (Gelaro et al. 2015, Figure 4.31), in which a deep warm-core tropical cyclone undergoing ET is shown.

Several mesoscale structures outside the deep tropics are generally missed or mis-represented in low-resolution global models. For example, high-latitude sub-synoptic scale vortices such as polar lows and Mediterranean tropical-cyclone like storms display similarities with tropical cyclones, including some level of vertical alignment, the presence of an eye-like feature, the prominent role played by convection, and latent and sensible total heat fluxes which can reach values comparable to hurricanes, albeit with larger contribution of sensible heat than latent heat (e.g., Reale and Atlas 2001; Rasmussen and Turner 2003). While the investigation of this type of event is outside the goal of this article and cannot be shown here, polar lows have been noted in the G5NR and they could therefore be targets for OSSEs. In fact, Putman (2015) shows the global distribution of tropical cyclone tracks obtained with a cyclone tracker which detects convective cyclones and requires, among other parameters, the presence of a warm core and vertical alignment. The tracker, aside from displaying purely tropical cyclones, shows some activity in the high latitudes, for example between Iceland and Greenland and on the Labrador Sea (Putman, his Figs. 1.13 and 1.14), where polar lows are often observed (e.g., Forsythe and Haynes 2015). The storms' intensities in the NR range predominantly within the tropical storm level.

Finally, evidence of realistic mesoscale convective complex (MCC) activity in the G5NR is provided by Putman (2015, his Fig. 1.16), showcasing the similarity between one observed MCC over the central US and one MCC produced by the G5NR, and also documenting a distribution of MCCs during the period May-June 2005-2006 in the NR, which compares well with composite geostationary IR observations (his Fig. 1.17).

4. Tropical Cyclone Activity and Structure in the G5 Nature Run

a. Tropical Cyclones in the Atlantic

With TCs the reasonable target of many future instruments, OSSEs have and will often be performed to investigate the potential use of such measurements to improve TC forecasts (e.g., Privé et al. 2014). For this reason, it is of paramount importance that TC activity, life cycle and structure are realistic in the NR. Following the same strategy which was previously adopted by Reale et al. (2007) to evaluate tropical cyclones in the ECMWF T511 NR, it is important to first verify that TCs occur in the G5NR not as sporadic or localized events, but as a realistic consequence of large-scale forcings in a manner comparable to reality. The preliminary step is to verify that the climatology of the main dynamical factors over the African Monsoon region and the tropical Atlantic is well represented. Modern-Era Reanalysis for Research and Applications, version 2 (MERRA-2), described and documented by Bosilovich et al. (2015a, b) and by Wargan and Coy (2016), is used for comparison. MERRA-2 is the new generation of the well-known MERRA (Rienecker et al. 2011) which has been successfully used, among many others, in studies concerning the meteorology of the African monsoon and tropical Atlantic region (e.g., Wu et al. 2012, Wu et al. 2013).

Figure 1 shows a meridional vertical cross-section of zonal wind at 0^o, comparing the NR in the July, August, and September (JAS) months of two different years with the corresponding MERRA-2 years. It is worth stressing that a comparison of monthly means cannot be interpreted as an actual seasonal forecasting validation. Since the NR is a free-running simulation constrained by SSTs and sea ice, and in which the memory of initial conditions is removed by the sufficiently long spin-up, a strict correspondence with observed means can not and should not be expected. It can only be noted that the NR represents the basic features of the African Monsoon circulation, namely: a) the Tropical Easterly Jet (TEJ), an upper-tropospheric jet located close to the Equator at about 100-200 hPa, b) the African Easterly Jet (AEJ) at about 600 hPa and peaking at about $12^oN - 16^oN$, c) the low-level westerly monsoonal flow confined below 800 hPa, and, d) the low-level easterly flow (also known as Harmatthan flow) at about 27^oN. The overall depiction of the AEJ in the NR is about 15% weaker than in MERRA-2, but it should be remembered that the AEJ depiction is affected by very large uncertainties, with differences of 20% in speed even among *state-of-the-art reanalyses* such as the ECMWF Reanalysis-40 (ERA-40), the National Centers for Environmental

Predictions, Reanalysis 2, (NCEP-R2), the Japanese 25-year Reanalysis (JRA-25) and MERRA, as discussed in detail in Wu et al. (2009) and in Wu et al. (2012). On the contrary, the representation of the Harmattan flow is stronger in the NR than in MERRA-2. However, since the Harmattan is a low-level, concentrated, easterly flow partly constrained by the orography of the Atlas range on its northern flank (e.g., Nicholson et al. 1996; Nicholson 2013), it is possible that the MERRA-2 coarser resolution hinders the Harmattan's representation in the reanalysis.

Aside from the intensity, the position of AEJ, TEJ and low-level monsoonal flow is very important because the cyclonically-sheared southward side of the AEJ (in which horizontal shear dominates) is conducive to barotropic instability at about the jet level, while the lower levels just below the AEJ (in which vertical shear dominates) are conducive to baroclinic instability. African Easterly Waves (AEWs) arise out of a combination of mechanisms: the presence of localized triggers, which can be convective in nature and may alter the vorticity and thermal profile of the atmosphere, and the favorable large-scale environment in which barotropic-baroclinic instability of the Charney-Stern type can occur (e.g., Kiladis et al. 2006; Hall et al. 2006; Thorncroft et al. 2008; Wu et al. 2012). Moreover, the presence of the TEJ, which is responsible for strong easterly shear and is generally unfavorable for development of vertically aligned structures, is an important forcing that confines the potential development of TCs to a narrow latitude range (just a few degrees south of the AEJ and north of the TEJ). The presence of all the fundamental elements of the African Monsoon region atmospheric circulation is a good preliminary assurance that the model may be capable of producing realistic weather patterns.

The next logical step is to verify whether the NR is able to produce realistic AEW activity. This is a complex issue because at least three types of AEWs are currently known: the 2.5-6 day waves developing to the south of the AEJ at about the jet level, the low-level baroclinic waves developing below the AEJ, and the less-known 6-9 day waves developing at the AEJ level, to the north of it. For a comprehensive discussion of various types of AEWs, see Wu et al. (2013). The AEWs that are more relevant to TC development are the 2.5-6 day waves developing to the south of the AEJ at about the jet level. In addition, the tracking or definition of AEWs may involve sophisticated objective methodologies (i.e., Berry et al. 2006) or the use of spectral techniques such as the Hilbert-Huang transform (Wu et al. 2013). However, a very simple and immediate way of detecting AEW activity is to plot a latitude-time Hovmøller diagram of the meridional component of the wind at, or slightly below, the jet level, and at a latitude south of the jet.

In Fig. 2 the 700 hPa Hovmøller of the meridional wind, obtained from the NR for the month of August 2005, is plotted for the latitude of $15^o N$ and for a longitude range spanning from $40^o W$ to $40^o E$, to be compared with the same quantity computed from MERRA-2 data. In Fig. 3 the same plot is produced for August 2006. The comparison between the NR and reanalyses in both years reveals that the amplitude, frequency and propagation speed of the AEWs is very similar. In particular, waves occur at a given longitude approximately every 3-6 days and propagate westward at a speed of about $5^o - 8^o d^{-1}$. Other features of the AEWs present in both the NR and MERRA-2 include: a) a discontinuity at about $15^o W$ where disturbances transition from land to ocean and, b) a pronounced diurnal cycle over the continent (evident by the horizontal lines on the easternmost side of the panels). Other realistic features are: a) occasional higher wind speeds, indicating the tendency of some AEWs to develop as TCs, b) upward curvatures (indicating acceleration) and c) disappearance (indicating either dissipation or disturbances which move to the north of the Hovmøller latitude). In general, higher detail and slightly more intense waves are present in the NR due to the higher resolution. The overall similarity between the AEW activity in the NR and in the reanalyses can be found in other months as well (e.g., July and September, not shown).

The next step is to investigate TC number, tracks, distribution and life cycles. Figure 4 shows the tracks and center pressure of TCs in the NR and in the observations for 2005. The corresponding

Table 1 shows the storm number, beginning and end dates for each storm, and the minimum center pressure. An important caveat is valid for this and all following figures containing TC tracks and corresponding TC tables for other basins. The storm detection algorithm applied to the NR involves thresholding parameters such as central pressure and presence of a warm core. The results are sensitive to the values of the 'thresholds'. In particular, it was found that less stringent thresholds in terms of warm-core intensity allow many more (weaker) depressions to be detected as TCs, especially over the Indian Ocean. For clarity, it was decided to use higher 'thresholds' in the tracker, concentrate on stronger storms, and use the same more-stringent criteria throughout all basins. This led to a slightly lower total number of TCs. Individual researchers can alter these criteria according to their needs, and may be able to detect a slightly higher number of TCs than the 17 TCs shown in Fig 4, by including some weak systems at a tropical depression intensity level. The choice of thresholds in the detecting algorithm also affects a TC's life span: a system undergoing transition can be categorized as extra-tropical (or still tropical) with a more (or less) stringent threshold. Since we have consistently used a stringent definition of TC, it should be noted that some TC tracks shown here could be prolonged if less restrictive tracking choices were to be adopted.

The observed 2005 TC tracks and center pressures for the Atlantic are obtained from the National Hurricane Center HURDATA2 best track (BT) database[1] which contains 6-hourly center pressure, winds, and location (Sampson and Schrader 2000). For consistency with other basins, retrospectively classified storms, which are available only in the Atlantic and east Pacific basins, are not included in this plot and table. Also, since weak storms are not tracked in the NR, non-developing depressions present in the database are ignored. Again for consistency with the storms tracked in the NR, only 'pure' TCs are plotted, and their extra-tropical transitions are not fol-

[1]available at http://www.nhc.noaa.gov/data/#hurdat

lowed. Because of these choices, four weak systems in the BT database (AL102005, AL192005, AL212005, AL232005) are not included in Table 1, so that the total number of observed 2005 Atlantic TCs is 27 instead of 31 as in the HURDATA2 database. Similar slight differences between the number of observed TCs listed in this article's tables and in the corresponding BT databases can be noted for other basins.

The comparison between NR and BT TCs shows that the TCs produced by the NR are less than the observed (17 versus 27, the latter number being an all-time record), but also indicates that the track distribution in the NR is very realistic (Figure 4). The majority of the TCs are of the Cape Verde type, moving across the Atlantic and recurving north. Two TCs originate in the Gulf of Mexico, leading to an overall realistic partition between Gulf and Atlantic systems (e.g., Asnani 2005). One system (G5NR 2005 TC 17) originate in the westerlies, which is typical for late-season hurricanes. It is particularly noteworthy that five G5NR TCs reach center pressures of less than 945 hPa, in good agreement with the observations for that year.

In contrast, the NR produces only 10 TCs in the 2006 season, which agrees closely with the 9 TCS observed in the much less active observed 2006 year (Fig .5). It should not be expected that a free-running model forced by SST and sea ice produces the same number of cyclones as in observations, since there are many factors controlling TC frequency other than SST. Moreover, as previously stated, the choice of the detection algorithm affects the TC number. However, it is important that model-generated natural variability does not contradict the observed variability. For reference, it should be noted that the ECMWF NR produced 12 TCs with 2005 SSTs (Reale et al. 2007).

The fact that the interannual variability in the NR has the same sign as the observed one suggests that SST alone, as reasonable to expect, exerts some control on TC number. As noted for 2005, the distribution of tracks in 2006 is realistic in the NR, with a majority of Cape Verde systems, and four storms forming in the Caribbean or in the Gulf.

In both years the TCs produced by the NR display a life time of a few days to less to almost two weeks. Individual tracks reveal singularities (i.e., discontinuous curvature changes) as well as binary interaction (i.e., two cyclones rotating around a common center with the stronger one moving slower, not shown), all features that are well known to forecasters and that frequently occur in the real atmosphere.

The final step in the investigation consists of examining the individual structure of the most intense storms taken at representative times.

Figure 6 shows a zonal vertical cross-section of wind and temperature across G5NR 2005 Atlantic TC no. 2 (see Fig. 4, hereafter G5NR-AL022005), taken at 1200 UTC 16 August 2005. The expected features of a mature hurricane can be noted: a vertically aligned structure, with wind speeds in excess of 65 ms^{-1}, a well-defined warm core (temperature anomaly greater than 12^{o}C), a scale on the order of few hundred km, a radius of maximum wind on the order of about 40-50 km, and a distinct eye-like feature with a relatively calm windless column. The overall structure is very realistic and represents an improvement with respect to the hurricanes seen in the previous ECMWF T511 NR (Reale et al. 2007, Fig. 4).

The realistic representation of G5NR-AL022005 is not an isolated occurrence in the NR. The subsequent Fig. 7 displays a snapshot of another 2005 hurricane in the NR: no. 12 (hereafter G5NR-AL122005) at a mature development stage. The vertical cross-section again displays realistic features: relatively calm central column, vertical alignment, scale on the order of hundreds of km, radius of maximum wind on the order of tens of km, and pronounced warm core. Interestingly, the snapshot depicting the strongest and most mature hurricane (Fig. 7), whose warm core temperature anomaly exceeds 14^{o}C, is also the one characterized by the tightest and most narrow eye-like feature. The same plot also shows the wind speed at the level of maximum wind, with the isotachs of 17 ms^{-1}, 25 ms^{-1} and 32 ms^{-1} super-imposed. To further appreciate the horizontal scales, a transect of sea level pressure and 10 m wind for the same storm is shown in Fig.8. The objective determination of TC scales from observations is a very complex problem that has been discussed, among others, by Chavas and Emanuel (2010), Knaff et al. (2014); Chan and Chan (2015) and Chan et al (2016). While the objective computation of scales for all TCs in the NR exceeds the purpose of this work, it can be stated that, for the storm noted in Figs. 7 and 8, the size appears within the observed range. Moreover, NR TC structures have been investigated at early stage of developments in the Atlantic and in other basins as well (not shown), finding an overall reduction of scale with intensification, a generally larger size for TCs in the western Pacific, in agreement with observations. e.g., Chavas et al. 2016) and also an increase in size with baroclinic transition (Gelaro et al. 2015, Fig. 4.31), also in agreement with observations (e.g. Hart and Evans 2001).

Another meaningful feature from an OSSE perspective is represented by precipitation structure. Teams designing future sensors to measure precipitation from space may be interested to perform OSSEs on TC-produced precipitation fields. TCs close to landfall in the NR can be qualitatively compared with radar imagery of observed storms whose tracks and intensity are similar. Figure 9 shows hourly accumulated precipitation produced by G5NR 2006 TC no. 4 (G5NR-AL042006), and the corresponding precipitation field from Katrina (2005), obtained NEXRAD data level 3 (one-hour precipitation totals). G5NR-AL042006 is chosen because of its track comparable to Katrina's one, and a landfall just to the east of New Orleans. The NR produces a reasonably realistic banded structure and an eye size comparable to Katrina's eye at landfall.

b. *Tropical Cyclones in the Eastern North Pacific*

The seasonal TC activity and the presence of interannual variability has been verified for all the other basins, paying special attention to the problems typically noted in global models. Especially for the Pacific, the impossibility of surface fluxes determined by prescribed SST to respond and adapt to the atmospheric forcings of the simulated TCs present some difficulties. In general, it is observed that a slow moving TC partially consumes the available heat energy in the underlying ocean, whereas in the G5NR a slow moving TC over a particularly warm ocean feature will have a constant energy source. Moreover, in the Pacific, mesoscale coupled ocean-atmosphere fluctuations associated with tropical instability waves add an additional level of complexity to the SST structure, which cannot be captured without a coupled system (e.g., Zhang and Busalacchi 2009; Zhang et al. 2014).

Figure 10 and Table 3 compare the eastern Pacific TC activity for 2005 in the NR and in observations, while Fig. 11 and Table 4 depict the corresponding 2006 activity. As for the Atlantic, some weak or after-analysis storms in the BT database are not included (EP162005 and EP022006, EP182006 and EP202006). Given the same caveats about the TC detecting and tracking algorithm previously noted, and the fact that by choosing a less restrictive definition of TC, a larger number of weak TCs and longer tracks could be detected, the Figures and Tables show that some level of interannual variability is reproduced by the NR, with more TCs in 2006. In fact, 2005 and 2006 observed TCs were 15 and 18 respectively, versus 8 and 19 in the NR. As for TC genesis, the most active region is between $90^o W$ and $120^o W$ and between $10^o N$ and $15^o N$ in both the NR and observations, with a predominant TC motion towards the west-north-west. However, the presence of outliers and TCs displaying erratic and/or retrograde motion with respect to the easterly flow, an aspect well known to forecasters and particularly frequent in 2006 (e.g., Pasch et al. 2009) is not captured very well by the NR, with NR TCs displaying less track variability than observed.

c. Tropical Cyclones in the western North Pacific Ocean

As noted for the eastern North Pacific, the absence of an atmosphere-ocean interaction in the G5NR is a limiting factor. However, in spite of the absence of air-sea interaction, which could be handled only by a fully coupled global model, it should be noted that some important atmospheric circulation elements, which were missing in previous NRs, are partially represented in the G5NR. Among these, the presence of features resembling westerly bursts is particularly remarkable. Figure 12 compares in matching Hovmøller diagrams the June, July and August 2006 zonal wind at the Equator from the NR (model level 70, nominal pressure of about 955 hPa) and from MERRA-2. Normally, a time-longitude plot of unfiltered Equatorial wind across the Pacific should reveal two sets of linear features which represent anomalies propagating in the midst of predominantly easterly flow: peaks of increased easterly speed which travel *within* the easterly flow, moving from east to west, and regions of decreased easterlies (or westerlies) which travel *against* the easterly flow, moving from west to east. When the magnitude of the decrease is stronger than the mean easterly flow, these regions of decreased easterlies appear as pulses of eastward-propagating westerly anomalies that are aptly named ‘westerly bursts’. Westerly bursts are associated with the Madden-Julian Oscillation (MJO, Madden and Julian 1971, 1972) but are strongly controlled by other factors, first and foremost the phase of the El Niño Southern Oscillation (ENSO). Transitioning ENSO can affect the ‘clean-ness’ of an MJO unfiltered signal. The 2005 and 2006 summers were not very representative in terms of the MJO signal, with the ENSO phase transitioning from positive to negative (2005) and then from negative to positive (2006). However, evidence of westerly bursts (i.e., eastward moving areas of westerly wind) is nevertheless clear in Fig. 12, particularly to the west of the Date Line. While the NR underestimated the westerlies' intensity, it is worth noting that only non-propagating stationary waves were detected by this team in other previous global non-coupled simulations (not shown). Being cyclonically-sheared on their northern flank, westerly bursts propagating along the Equator are among the factors that can contribute to increased low-level cyclonic vorticity and therefore to TC-genesis over the western North Pacific (e.g., Hogsett and Zhang 2010; Shu and Zhang 2015).

Aside from clear evidence of westerly bursts, the overall complex interaction between the tropical and extra-tropical atmosphere over the western North Pacific leads to a very large variability of extra-tropical (ET) transition patterns, well documented in literature (e.g., Harr and Dea 2009). Figure 13 and Table 5 demonstrate that the overall TC activity in the NR is reasonable, with 23 TCs instead of 25 observed. The observed TC tracks and center pressures for the western North Pacific, Indian Ocean and Australian basins are obtained from the Joint Typhoon Warning Center (JTWC).[2] The majority of the TC genesis points occurs between 130^oE and 170^oE and 10^oN and 20^oN, indicating that there is a general inability of the model to produce TCs close to the Equator, possibly because of the weaker than observed eastward propagation of westerly bursts as noted in Fig 12) and higher than observed vertical shear (not shown). A similar situation is noted for 2006 (Fig. 14and Table 6) with 21 simulated TCs against 26 observed. In terms of track distribution, both years show a predominance of west-north-westward tracks with landfall over Philippines and China, and a tendency of northward and northeastward recurvatures north of 25^oN. It can be confidently stated that the model reproduces the overall range in track variability.

As for intensity, several TCs in both NR seasons reach center pressure well below 950 hPa. Of particular interest is the intensity of one G5NR typhoon in the 2005 season, and two in the 2006

[2] available at http://www.usno.navy.mil/NOOC/nmfc-ph/RSS/jtwc/best_tracks/index.html

season (Tables 5 and 6) whose center pressure goes below 920 hPa. However, no TC in the NR reaches the most extreme observed value of 898 hPa recorded in both 2005 and 2006.

G5NR 2006 western North Pacific TC no. 3 (hereafter G5NR-WP032006, following the JTWC naming conventions) is selected for further investigation. Figure 15 shows the meridional and zonal cross-sections at peak intensity, when center pressure reached the remarkable value, for a global model, of 906 hPa. The cross-sections indicate a high degree of symmetry with a very well-defined eye, a warm core temperature anomaly greater than 14^oC, winds exceeding $75 m s^{-1}$ on all four quadrants, and a radius of maximum wind on the order of about 40 km.

d. Tropical Cyclones in the North Indian Ocean

The North Indian Ocean is arguably the most difficult basin for TC forecasting. Aside from well-studied cases in which even the objective analysis of already existing TCs failed to represent TC circulations, as in the infamous 2008 case of Nargis, discussed in Reale et al. (2009), free-running models examined by this team have produced totally inactive North Indian Ocean TC seasons without a single storm, and seasons in which up to 40 TCs were simulated. These unrealistic excesses are probably caused by the extreme sensitivity of any model to small changes in the circulation. In fact, the SSTs over the Indian Ocean are extremely warm (often more than 30^oC but the environment is not generally conducive to TC development because of the very strong shear. In fact, during the summer, the combination of the Somali Jet (SJ), southwesterly flow peaking at about 900 hPa, which is particularly important in modulating the Indian Monsoon phases (e.g., Krishnamurti et al. 1976, Halpern and Woiceshyn, 2001) and the TEJ, easterly flow peaking at about 150 hPa, (e.g., Chen and van Loon 1987, Nicholson et al. 2007), creates zonal shear values of up to $-40\ m s^{-1}$ or more. In spite of the huge latent and sensible heat fluxes, and the environment being extremely conducive to convection, cyclonic circulations cannot generally overcome the vertical shear except that in rare situations when the shear relaxes. Then very sudden development can occur. In other cases TCs can only maintain shallow structures and any upper-level development is eroded above 300 hPa by the upper-level easterly flow. In this environment, which essentially has a surplus of energy available but hostile dynamical forcings, small errors in the representation of the shear can lead to large errors in the estimate of TC activity. At the same time, long simulations have suggested that TC activity over this region is very sensitive to the model in convective parametrizations. It has been customary for this team, while analyzing previous long simulations, in addition to finding simulated TC activity over the North Indian Ocean ranging from totally inactive to unrealistically hyperactive, to spot simulated TCs in locations where they have never been detected (not shown).

With this preliminary discussion, it is now easier to place into context the representation of TC activity in the G5NR over the North Indian Ocean. Figures 16 and 17 compare the representation of the Somali Jet in 2006 (2005 is not significantly different, not shown). It can be noted that the predominantly easterly flow over the Southern Hemisphere is deflected northward and then northeastward by the combining effect of the Indian monsoon low and the orography of eastern Africa, in agreement with observations and other modeling studies (e.g., Chakraborty et al. 2009). The higher resolution of the G5NR allows a sharper depiction of the SJ than MERRA-2, including the well-known bifurcation caused by the 'Horn of Africa'. Most interesting is the SJ vertical structure. From aircraft measurements acquired during campaigns such as Monsoon Experiment (MONEX 79; e.g., Holt and Sethuraman 1985) it is known that the SJ is a very shallow feature, peaking at about $10^oN - 15^oN$ and about 875 hPa and disappearing at about 600 hPa. These features are clearly represented in Fig. 17 and are confirmed by the reanalysis. Also noteworthy are the secondary westerly mid-tropospheric maximum present in the reanalysis at about the Equator (which was not detected by this team in any previous long global simulations) and the excellent depiction of the TEJ above 200 hPa.

Probably because of the overall realistic rendering of the *mean* SJ and TEJ in the NR, the representation of the North Indian Ocean TC activity, while still not optimal, is definitely improved with respect to previous long simulations. Figures 18 and 19, and Table 7, show a total TC number of 4 simulated versus 7 observed in 2005, and 6 simulated versus 7 observed in 2006 (including Typhoon Dorian which crossed the Malay Peninsula from the Pacific becoming the 7th North Indian Ocean TC for the season).

However, the distribution of TC locations and their tracks differ significantly between the NR and observations, and the fundamentally erratic nature of TC tracks over that basin does not appear to be fully captured. In 2005, observed TC tracks seem to 'radiate' from the center of the Bay of Bengal in almost all directions, and that variability is not reproduced by the G5NR. A somehow larger track variability, closer to the observed one, is noted in the 2006 G5NR season. As noted previously, very small lapses in the shear can very quickly trigger a TC genesis process, which limits the overall predictability of northern Indian Ocean TC activity.

In terms of vertical structure, the NR displays a significant number of poorly developed systems, or systems fighting against shear, in agreement with climatology (not shown).

e. Tropical Cyclones in the South Indian Ocean

The southern Indian Ocean is conventionally treated by the Joint Typhoon Warning Center (JTWC) as one of the two basins of the Southern Hemisphere season with the other being the South Pacific basin, having the longitude of 135^oE as separator between the two (e.g., Lander and Guard 2001). However, the TCs affecting the eastern part of the South Indian Ocean are more often regarded as TCs affecting the Australian region. This article follows the latter convention and plots the TCs over the eastern and western portions of the South Indian ocean separately.

Figures. 20 and 21, and Tables 8 and 9 compare the TCs that formed over the South Indian Ocean (west of $100^{o}E$) in the G5NR and in the observations. Specifically, observed TCs 1 to 9 correspond to TCs numbered in the JTWC BT database as 1, 2, 3, 4, 9, 12, 14, 16 and 22 in 2005-2006, and to TCs 3, 5, 6, 10, 13, 14, 15, 16, 19 and 22 in 2006-2007, respectively.

The NR produces a very realistic activity, substantially better than over the North Indian Ocean, not just in terms of overall number, but also in terms of track distribution. TCs generally form between $5^{o}S$ and $15^{o}S$ (except for a few originating west of Madagascar), track southward or westward, gradually recurving eastward under the influence of the westerly flow, and display frequent singularities in their tracks, such as loops, sharp recurvatures and binary interactions. The NR exhibits a very convincing spectrum of TC tracks over this basin. A remarkable TC occurred during the 2006-2007 NR South Indian Ocean season is investigated (TC no. 5 in Fig 21). Because of its exceptional symmetry, both meridional and zonal vertical cross-sections of wind and temperature across the TC, at a mature stage, are shown in Fig. 22, which demonstrates the consistency in TC structures produced by the NR over *all* basins. This particular system is noteworthy, aside from its symmetry and pronounced warm core, because of its winds which exceed 70 ms^{-1} on each quadrant. The eye is very well defined, the radius of maximum wind is on the order of 40 km. Its central pressure reaches 919 hPa. However, as noted for the western North Pacific basin, some observed cyclones reach even deeper values (observed TC no.2 in 2006-2007, 904 hPa).

f. Tropical cyclones in the Australian region

Tropical cyclones over the eastern Indian Ocean and southwestern Pacific are traditionally studied together as TCs of the Australian region. As noted by Hall et al. (2001) the entire northern

Australian coastline is affected by landfalls and there are two main cyclogenesis area: a western one in the Indian Ocean and the Timor Sea, and an eastern one in the Pacific (Coral Sea). Moreover, there are cases of Pacific TCs regenerating in the Indian Ocean after having crossed land (e.g., McBride and Keenan 1982). The comprehensive climatological assessment of TCs in the Australian region by Dare and Davidson (2004), including 500 cases and spanning 40 years, describes, in addition to the eastern and western regions, a third cyclogenetic area to the north of the Australian coastline at about 135^oE. Among the prominent factors affecting the Australian region TC season are the proximity between the Inter Tropical Convergence Zone (ITCZ) and the mid-latitude storm track, the presence of a large land mass and an overall monsoonal environment (e.g., McBride and Keenan 1982; Holland 1984; Dare and Davidson 2004). Other important forcings are the phase of ENSO (e.g., Nicholls 1979; Solow and Nicholls 1990; Catto et al 2012) and the MJO activity (e.g., Hall et al. 2001). The overall track variability appears to be larger than the Atlantic or the Pacific and the proximity of the genesis region in the ITCZ to the coastline can lead to difficult landfall forecasts.

In spite of the complexity, the G5NR performs satisfactorily over the region. In Fig. 23 and Table 10 the comparison between TCs observed in the 2005-2006 season and the ones produced by the G5NR is provided. As noted before, the JTWC BT database is split into two, to treat separately the South Indian Ocean from the Australian Region. Therefore the 14 observed TCs listed in Table 10 correspond, in the JTWC BT database, to TCs 5, 6, 7, 8, 10, 11, 13, 15, 17, 18, 19, 20, 21 and 23 for 2005-2006, and to TCs 1, 2, 4, 7, 8, 9, 11, 12, 17, 18, 20, 21, 23 and 24 for 2006-2007.

Two of the three known cyclogenetic regions appear to be present in the simulations, and the overall track distribution appears to be realistic, including retrograde motion and multiple landfalls with regeneration, which is common for TCs originating close to the coastline. A similar situation can be noted in the 2006-2007 season (Fig. 24 and Table 11).

The intensity range is quite reasonable with several NR TCs reaching values lower than 950 hPa during both seasons, in agreement with observations. Somewhat perplexing is the persistence of relatively deep storms inland in the NR, possibly because of insufficient surface drag.

5. Conclusions

OSSEs are a labor-consuming and computer-intensive methodology and benefit from large collaborative efforts. An essential element for OSSEs is the NR, which needs to satisfy a number of requirements to enable realistic OSSE results.

The previous widely used NR produced by the ECMWF has served the OSSE community for a decade, thanks to its outstanding qualities. However, because of the growth in computer power, modeling developments, and improved observing systems, the need for a new NR has become apparent.

In recent years, in an attempt to provide a NR usable in state-of-the-art OSSEs, the NASA GMAO has produced and evaluated several runs with a configuration similar to the ECMWF T511 NR, but at increasingly higher resolution and extending the integration length to two years. One example of this type of effort is the 14-km horizontal resolution 2-year simulation documented by Putman and Suarez (2011), which represented an important milestone, because it generated, in addition to a climatologically realistic total number of TCs, also a very satisfactory interannual variability in TC activity between 2005 and 2006. Multiple evaluation teams have assessed this and other long simulations as candidate next-generation NRs, paying attention, among several other concerns, to the realism of TC activity.

After substantial modeling development the NASA GMAO has finally released for use in OSSEs a 7-km NR which stems from a large collaborative effort, several years of preparation and which has been subjected to an extensive evaluation (Gelaro et al. 2015).

The goal of this article is to evaluate the suitability of the G5NR to serve as a NR for OSSEs focused on future instruments targeting TCs. The evaluation is phenomenological and event-focused, and includes comparisons with reanalyses and observed tropical cyclone best track information. As is the case for all evaluations focused on a NR, no direct correspondence with observed events can be expected, but the specific events investigated must fall within an acceptable range of observed variability and realism.

This article investigates TC activity in all basins: Atlantic, eastern North Pacific, western North Pacific, North Indian Ocean, South Indian Ocean and Australian Region. The investigation shows that the TC activity lies well within the spectrum of observed activity in all basins and also displays a satisfactory degree and sense of variability between the two years. This article also shows that tropical cyclone structure is well represented, with very clear eye features of reasonable scale. The intensity is also very realistic for the resolution of 7km, with center pressures reaching values down to 906 hPa and wind speeds often in excess of $75 m s^{-1}$. Finally, evidence is provided that the NR TC activity arises out of realistic forcings, and that the major dynamical factors controlling tropical weather are well represented.

The evaluation documented in this article confirms that the 7km G5NR provides a significant advance with respect to previous long simulations produced for OSSEs, and may represent a valuable tool to perform OSSEs focused particularly on future instruments or missions designed to investigate TCs and other high-impact weather systems, such as, but not limited to, CYGNSS. While the 7km resolution may still be not sufficient for certain very high resolution applications investigating future instruments focused on eyewall replacement cycles, the evidence provided suggests that the 7km G5NR could be an excellent framework for further downscaling.

Acknowledgments. The GEOS-5 Atmospheric General Circulation Model development in the Global Modeling and Assimilation Office is funded by David Considine, under the NASA's Modeling, Analysis and Prediction (MAP) program. The authors thank Dr. Ross Hoffman and one anonymous reviewer for helpful suggestions.

References

Andersson, E., and M. Masutani (2010), Collaboration on observing system simulation experiments (Joint OSSE), ECMWF Newsl., No. 123, pp. 1416, ECMWF, Reading, U. K. Available online at `http://www.emc.ncep.noaa.gov/research/JointOSSEs/publications/JOSSE-Publication-files/Andersson_JOSSE_ECMWF_News_No123.pdf`

Annane, B., B. McNoldy, J. Delgado, L. Bucci, R. Atlas, and S. Majumdar, 2015: CYGNSS data and surface wind analysis. 19th Conference on Integrated Observing and Assimilation Systems for the Atmosphere, Oceans, and Land Surface (IOAS-AOLS), American Meteorological Society, Boston, MA, Phoenix, AZ, poster 238. Manuscript and handout Available online at: `https://ams.confex.com/ams/95Annual/webprogram/Paper251064.html`

Arnold, C., and C. Dey, 1986: Observing-systems simulation experiments: Past, present, and future. *Bull. Amer. Meteor. Soc.*, **67,** 687695, doi:10.1175/1520-0477(1986)067<0687:OSSEPP>2.0.CO;2.

Asnani, G. C., 2005: *Tropical Meteorology*. Publisher: Indian Institute of Tropical Meteorology, Pashan, Pune-411008, India. 3 vols.

Atlas, R., 1997: Atmospheric observations and experiments to assess their usefulness in data assimilation, *J. Meteorol. Soc. Jpn.*, **75(1B),** 111 130.

Atlas, R., E. Kalnay, and M. Halem, 1985: Impact of satellite temperature soundings and wind data on numerical weather prediction. *Opt. Eng.*, **24,** 341-346, doi:10.1117/12.7973481.

—, R. N. Hoffman, Z. Ma, G. D. Emmitt, S. A. Wood Jr., S. Greco, S. Tucker, L. Bucci, B. Annane, R. M. Hardesty, and S. Murillo, 2015: Observing System Simulation Experiments (OSSEs) to Evaluate the Potential Impact of an Optical Autocovariance Wind Lidar (OAWL) on Numerical Weather Prediction. *J. Atmos. Oceanic Technol.*, **32,** 15931613.

Berry, G., Thorncroft, C. and Hewson, T. 2006: African easterly waves in 2004 Analysis using objective techniques. *Mon. Wea. Rev.*, **133,** 752-766.

Bosilovich, M. G., R. Lucchesi, and M. Suarez, 2015a. MERRA-2: File Specification. GMAO Office Note No. 9 (Version 1.1). [Available online at https://gmao.gsfc.nasa.gov/pubs/docs/Bosilovich785.pdf]

Bosilovich, M. G., and Coauthors, 2015b: MERRA-2: Initial evaluation of the climate. Series on Global Modeling and Data Assimilation Tech. Rep. NASA/TM2015-104606, Vol. 43, 145 pp. [Available online at http://gmao.gsfc.nasa.gov/reanalysis/MERRA-2/docs/.]

Catto, J. L., N. Nicholls, and C. Jakob, 2012: North Australian Sea Surface Temperatures and the El NiñSouthern Oscillation in Observations and Models. *J. Climate*, **25,** 50115029.

Chakraborty, A., Nanjundiah, R. S. and Srinivasan, J., 2009: Impact of African orography and the Indian summer monsoon on the low-level Somali jet. *Int. J. Climatol.*, **29,** 983992. doi: 10.1002/joc.1720

Chan, K. T., and J. C. Chan, 2015: Global climatology of tropical cyclone size as inferred from QuikSCAT data. *Int. J. Climatol.*, **35,** 48434848, doi:10.1002/joc.4307.

Chavas, D. R., and K. A. Emanuel, 2010: A QuikSCAT climatology of tropical cyclone size. *Geophys. Res. Lett.*, **37,** L18816, doi:10.1029/2010GL044558.

—, N. Lin, W. Dong, and Y. Lin, 2016: Observed tropical cyclone size revisited. *J. Climate*, **29,** 29232939, doi:10.1175/JCLI-D-15-0731.1.

Chen, T-C., and H. van Loon, 1987: Interannual variation of the tropical easterly jet. *Mon. Wea. Rev.*, **115,** 17391759.

Chin, M., P. Ginoux, S. Kinne, O. Torres, B. N. Holben, B. N. Duncan, R. V. Martin, J. A. Logan, A. Higurashi, and T. Nakajima, 2002: Tropospheric Aerosol Optical Thickness from the GOCART Model and Comparisons with Satellite and Sun Photometer Measurements. J. Atmos. Sci., **59,** 461483.

Colarco, P., A. da Silva, M. Chin, and T. Diehl, 2010: Online simulations of global aerosol distributions in the NASA GEOS-4 model and comparisons to satellite and ground-based aerosol optical depth. *J. Geophys. Res.*, **115,** D14207, doi:10.1029/2009JD012820.

da Silva, A.M., W. Putman, and J. Natalla, 2015. File Specification for the 7-km GEOS-5 Nature Run, Ganymed Release (Non-hydrostatic 7-km Global Mesoscale Simulation). GMAO Office Note No. 6, 72 [Available online at: ttps://gmao.gsfc.nasa.gov/pubs/office_notes/]

Dare, R. A., and N. E. Davidson, 2004: Characteristics of Tropical Cyclones in the Australian Region. *Mon. Wea. Rev.*, **132,** 30493065. doi: http://dx.doi.org/10.1175/MWR2834.1

Draper, C., R. Cullather, R. Koster, G. Vernieres, and Y. Vikhlieave, 2015: Surface Characteristics, *Evaluation of the 7-km GEOS-5 Nature Run.* NASA/TM-2014-104606, Vol **36,** 153-191.

Forsythe, J. M., and J. M. Haynes, 2015: CloudSat Observes a Labrador Sea Polar Low. *Bull. Amer. Meteor. Soc.*, **96,** 12291231, doi: 10.1175/BAMS-D-14-00058.1.

Gelaro, R., and co-authors, 2015: *Evaluation of the 7-km GEOS-5 Nature Run.* NASA/TM-2014-104606, Vol **36,** 285 p. [Available online at: `https://gmao.gsfc.nasa.gov/pubs/docs/Gelaro736.pdf`.]

Hall, J. D., A. J. Matthews, and D. J. Karoly, 2001: The Modulation of Tropical Cyclone Activity in the Australian Region by the MaddenJulian Oscillation. *Mon. Wea. Rev.*, **129,** 29702982.

Hall, N. M. J., G. N. Kiladis, and C. D. Thorncroft, 2006: Three-Dimensional Structure and Dynamics of African Easterly Waves. Part II: Dynamical Modes. *J. Atmos. Sci.*, **63,** 2231-2245.

Halpern, D., and P. M. Woiceshyn, 2001: Somali Jet in the Arabian Sea, El Niño, and India Rainfall. *J. Climate,* **14,** 434441.

Harr, P. A. and J. M. Dea 2009: Downstream development associated with the extratropical transition of tropical cyclones over the western north Pacific. *Mon. Wea. Rev.*, **137,** 1295-1319.

Hart, R. E., and J. L. Evans, 2001: A climatology of the extratropical transition of Atlantic tropical cyclones. *J. Climate,* **14,** 546564, doi:10.1175/1520-0442(2001)014<0546:ACOTET>2.0.CO;

Hoffman, R. N., C. Grassotti, R. G. Isaacs, J.-F. Louis, and T. Nehrkorn, 1990: Assessment of the impact of simulated satellite lidar wind and retrieved 183 GHz water vapor observations on a global data assimilation system. *Mon. Wea. Rev.,* **118,** 25131542.

—, and R. Atlas, 2016: Future Observing System Simulation Experiments. *Bull. Amer. Meteor. Soc.*, doi:10.1175/BAMS-D-15-00200.1, in press.

Hogsett, W., and D.-L. Zhang, 2010: Genesis of Typhoon Chanchu (2006) from a Westerly Wind Burst Associated with the MJO. Part I: Evolution of a Vertically Tilted Precursor Vortex, *J. Atmos. Sci.,* **67,** 37743792, doi:10.1175/2010JAS3446.1.

Holland, G. J., 1984: On the climatology and structure of tropical cyclones in the Australian/southwest Pacific region: I. Data and tropical storms. *Aust. Meteor. Mag.*, **32,** 115.

Holt, T., and S. SethuRaman, 1985: Aircraft and ship observations of the mean structure of the marine boundary layer over the Arabian Sea during MONEX 79. *Boundary-Layer Met.*, **33,** 259282.

Kiladis, G. N., C. D. Thorncroft, and N. M. J. Hall, 2006: Three-Dimensional Structure and Dynamics of African Easterly Waves. Part I: Observations, *J. Atmos. Sci.,* **63,** 2212-2230.

Kleist, D. T., and K. Ide, 2015: An OSSE-Based Evaluation of Hybrid VariationalEnsemble Data Assimilation for the NCEP GFS. Part I: System Description and 3D-Hybrid Results. *Mon. Wea. Rev.,* **143,** 433451.

Kocin, P. J., and L. W. Uccellini, 2005: *Northeast Snowstorms.* Vols. 1 and 2, Meteor. Monogr., No. 54, Amer. Meteor. Soc., 818 pp.

Knaff, J. A., S. P. Longmore, and D. A. Molenar, 2014: An objective satellite-based tropical cyclone size climatology. *J. Climate,* **27,** 455476, doi:10.1175/JCLI-D-13-00096.1

Krishnamurthy, T. N., J. Molinari, and H.-L. Pan, 1976: Numerical Simulation of the Somali Jet *J. Atmos. Sci.,* **33,** 23502362.

Kyle G. S., L. F. Bosart, 2014: The Extratropical Transition of Tropical Cyclone Edisoana (1990). *Mon. Wea. Rev.,* **142,** 27722793.

Lander M. A., and C. P. Guard, 2001: Western North Pacific, North Indian Ocean, and Southern Hemisphere Tropical Cyclones of 1997. *Mon. Wea. Rev.,* **129,** 30153036.

Ma, Z., L. P. Riish/ojgaard, M. Masutani, J. S. Woollen, and G. D. Emmitt, 2015: Impact of Different Satellite Wind Lidar Telescope Configurations on NCEP GFS Forecast Skill in Observing System Simulation Experiments. *J. Atmos. Oceanic Technol.,* **32,** 478495.

Madden, R. A. and P. R. Julian, 1971: Detection of a 4050-day oscillation in the zonal wind in the tropical Pacific. *J. Atmos. Sci.,* **28**, 702708.

—, and —, 1972: Description of global-scale circulation cells in the tropics with a 4050 day period. *J. Atmos. Sci.,* **29,** 11091123.

Masutani, M. K., and Coauthors, 2010: Observing system simulation experiments at the National Centers for Environmental Prediction. *J. Geophys. Res.*, **115,** D07101, doi:10.1029/2009JD012528.

McBride, J. L., and T. D. Keenan, 1982: Climatology of tropical cyclone genesis in the Australian region. *J. Climatol.*, **2,** 1333

McCarty, W., R. M. Errico, R. Gelaro, 2012: Cloud coverage in the Joint OSSE Nature Run. *Mon. Wea. Rev.*, **140,** 1863-1871.

Molod, A., M.-J. Kim, J. Nattala, M. Bosilovich, S. Schubert, and W. Chao, 2015: Wind and Temperature, *Evaluation of the 7-km GEOS-5 Nature Run.* NASA/TM-2014-104606, Vol **36,** 67-112.

Nicholls, N., 1979: A possible method for predicting seasonal tropical cyclone activity in the Australian region. *Mon. Wea. Rev.*, **107,** 12211224.

Nicholson, S. E., 1996: Africa. *Encyclopedia of Climate and Weather,* S. H. Schneider, Ed., Simon and Schuster, 1319.

—, A. I. Barcilon, M. Challa, J. Baum, 2007: Wave Activity on the Tropical Easterly Jet. *J. Atmos. Sci.*, **64,** 27562763.

—, 2013: The West African Sahel: A Review of Recent Studies on the Rainfall Regime and Its Interannual Variability. *ISRN Meteorology*, **vol. 2013,** Article ID 453521, 32 pp., doi:10.1155/2013/453521

Nolan, D. S., R. Atlas, K. T. Bhatia, and L. R. Bucci (2013), Development and validation of a hurricane nature run using the joint OSSE nature run and the WRF model, *J. Adv. Model. Earth Syst.*, **5,** 382405, doi:10.1002/jame.20031.

Norris, P., W. McCarty, and R. Errico, 2015: Clouds and Radiation, *Evaluation of the 7-km GEOS-5 Nature Run.* NASA/TM-2014-104606, Vol **36,** 192-112.

Ott, L., A. Darmenov, A. da Silva, V. Buchard, and K. Wargan, 2015: Aerosol and Trace Gases, *Evaluation of the 7-km GEOS-5 Nature Run.* NASA/TM-2014-104606, Vol **36,** 243-275.

Pasch, R. J., and Coauthors, 2009: Eastern North Pacific hurricane season of 2006. *Mon. Wea. Rev.,* **137,** 320, doi:10.1175/2008MWR2508.1.

Privé, N. C., R. Errico, and K.-S. Tai, 2013a: The impact of increased frequency of rawinsonde observations on forecast skill investigated with an Observing System Simulation Experiment *Mon. Wea. Rev.,* **142,** 18231834.

—, —, , and —, 2013b: Validation of the forecast skill of the global modeling and assimilation office Observing System Simulation Experiment. *Q. J. Roy. Met. Soc.,* **139,** 13541363.

—, Y. Xie, J. S. Woollen, et al. 2013c: Evaluation of the Earth Systems Research Laboratorys global Observing System Simulation Experiment system. *Tellus-A,* **65,** doi:http://dx.doi.org/10.3402/tellusa.v65i0.19011.

—, —, S. Koch, R. Atlas, S. J. Majumdar, and R. N. Hoffman, 2014: An observing System Simulation Experiment for the Unmanned Aircraft System Data Impact on Tropical Cyclone Track Forecasts. *Mon. Wea. Rev.,* **142,** 4357-4363.

—, Coy, L., and R. M. Errico, 2015: Wind and Temperature, *Evaluation of the 7-km GEOS-5 Nature Run.* NASA/TM-2014-104606, Vol **36,** 30-66.

Putman, W. M., and S.-J. Lin, 2007: Finite-volume transport on various cubed-sphere grids. *J. Comp. Phys.,* **227** (2007), 55-78.

—, and M. Suarez, 2011: Cloud-system resolving simulations with the NASA Goddard Earth Observing System global atmospheric model (GEOS-5), *Geophys. Res. Lett.,* **38,** L16809, doi:10.1029/2011GL048438.

—, 2015: Overview. *Evaluation of the 7-km GEOS-5 Nature Run.* NASA/TM-2014-104606, Vol **36,** 1-29.

Rasmussen, E. A., and Turner, J., 2003: *Polar Lows: Mesoscale Weather Systems in the Polar Regions*, Cambridge: Cambridge University Press, p. 612, ISBN 0-521-62430-4.

Reale, O., and R. Atlas, 2001: Tropical Cyclone-like Vortices in the Extratropics: Observational Evidence and Synoptic Analysis. *Wea. Forecasting*, **16,** 7-34.

—, J. Terry, M. Masutani, E. Andersson, L. P. Riishojgaard, J. C. Jusem, 2007: Preliminary evaluation of the European Centre for Medium-Range Weather Forecasts (ECMWF) Nature Run over the Tropical Atlantic and African Monsoon region. *Geophys. Res. Lett.*, **34**, L22810, doi:10.1029/2007GL31640.

—, W. K. Lau, J. Susskind, E. Brin, E. Liu, L. P. Riishojgaard, M. Fuentes, R. Rosenberg, 2009: AIRS Impact on the Analysis and Forecast Track of Tropical Cyclone Nargis in a global data assimilation and forecasting system. *Geophys. Res. Lett.*, 36, L06812, doi:10.1029/2008GL037122.

—, W. K. Lau, and A. da Silva, 2011: Impact of interactive aerosol on the African Easterly Jet in the NASA GEOS-5 global forecasting system. *Wea. Forecasting*, **26,** 504-519.

—, K. M. Lau, A. da Silva, and T. Matsui, 2014: Impact of assimilated and interactive aerosol on tropical cyclogenesis. *Geophys. Res. Lett.*, **41,** 3282-3288, doi:10.1002/2014GL059918.

Rienecker, M. M., and Coauthors, 2011: MERRA: NASAs Modern-Era Retrospective Analysis for Research and Applications. *J. Climate*, **24,** 36243648, doi:10.1175/JCLI-D-11-00015.1.

Sampson, C. R., and A. J. Schrader, 2000: The Automated Tropical Cyclone Forecasting System (Version 3.2). *Bull. Amer. Meteor. Soc.*, **81,** 1231-1240.

Solow, A. and N. Nicholls, 1990: The Relationship between the Southern Oscillation and Tropical Cyclone Frequency in the Australian Region. *J. Climate*, **3,** 10971101.

Shu, S., and F. Zhang, 2015: Influence of equatorial waves on the genesis of super typhoon Haiyan (2013). *J. Atmos. Sci.*, **72,** 45914613.

Sinclair, M. R., 1993: Synoptic-scale diagnosis of the extratropical transition of a southwest Pacific tropical cyclone. *Mon. Wea. Rev.,* **121,** 941960.

Thorncroft, C. D., J. Hall, and G. N. Kiladis, 2008: Three-dimensional structure and dynamics of African easterly waves. Part III: Genesis. *J. Atmos. Sci.,* **65,** 35963607.

Wargan, K. and L. Coy, 2016: Strengthening of the Tropopause Inversion Layer during the 2009 Sudden Stratospheric Warming: A MERRA-2 Study. *Journal of the Atmospheric Sciences,* **73,** 18711887, doi: 10.1175/JAS-D-15-0333.1

Wu, M.-L, O. Reale, S. Schubert, M. J. Suarez, R. Koster, P. Pegion, 2009: African Easterly Jet: Structure and Maintenance. *J. Climate*, **22**, 4459-4480.

—, —, —, —, C. Thorncroft, 2012: African Easterly Jet: barotropic instability, waves and cyclogenesis. *J. Climate*, **25,** 1489-1510.

—, —, —, 2013: A characterization of African Easterly Waves on 2.5-6 and 6-9 day time scales. *J. Climate*, **26,** 6750-6774.

Zhang, R.-H., and A. J. Busalacchi, 2009: An empirical model for surface wind stress response to SST forcing induced by tropical instability waves (TIWs) in the eastern equatorial Pacific. *Mon. Wea. Rev.,* **137,** 20212046, doi:10.1175/2008MWR2712.1.

—, 2014: Effects of tropical instability wave (TIW)-induced surface wind feedback in the tropical Pacific Ocean. *Clim. Dyn.,* **42,** 467-485. doi:10.1007/s00382-013-1878-6

LIST OF TABLES

Table 1. Simulated (NR) and observed (BT) TCs, 2005 Atlantic Season. 40

Table 2. Simulated (NR) and observed (BT) TCs, 2006 Atlantic Season. 41

Table 3. Simulated (NR) and observed (BT) TCs, 2005 East Pacific Season. 42

Table 4. Simulated (NR) and observed (BT) TCs, 2006 East Pacific Season. 43

Table 5. Simulated (NR) and observed (BT) TCs, 2005 North West Pacific Season. . . . 44

Table 6. Simulated (NR) and observed (BT) TCs, 2006 North West Pacific Season. . . . 45

Table 7. Simulated (NR) and observed (BT) TCs, North Indian Ocean Seasons: 2005 (above) and 2006 (below) 46

Table 8. Simulated (NR) and observed (BT) TCs, 2005-2006 South Indian Ocean Season. 47

Table 9. Simulated (NR) and observed (BT) TCs, 2006-2007 South Indian Ocean Season. 48

Table 10. Simulated (NR) and observed (BT) TCs, 2005-2006 Australian Region Season. . . 49

Table 11. Simulated (NR) and observed (BT) TCs, 2006-2007 Australian Region Season. . . 50

ATLANTIC OCEAN 2005				
NATURE RUN			BEST TRACK	
TC No.	Start - end date (mmdd hh:hh)	Min SLP (hPa)	Start - end date (mmdd hh:hh)	Min SLP (hPa)
1	0803 15:00 - 0812 05:00	948	0608 18:00 - 0614 06:00	989
2	0813 19:00 - 0817 22:30	931	0628 18:00 - 0630 00:00	1002
3	0822 21:00 - 0825 15:00	972	0703 18:00 - 0711 06:00	991
4	0826 10:00 - 0828 14:30	975	0704 18:00 - 0718 06:00	930
5	0830 13:30 - 0903 22:00	972	0711 00:00 - 0721 12:00	929
6	0904 22:00 - 0916 03:00	938	0721 18:00 - 0731 00:00	997
7	0907 08:00 - 0910 18:30	966	0723 18:00 - 0725 18:00	1005
8	0911 06:00 - 0914 21:00	952	0802 18:00 - 0814 00:00	994
9	0915 00:00 - 0922 13:30	939	0804 18:00 - 0818 12:00	970
10	0915 23:30 - 0923 01:30	951	0822 12:00 - 0823 12:00	998
11	0916 19:30 - 0928 19:30	962	0823 18:00 - 0831 06:00	902
12	0921 04:00 - 0926 09:00	925	0828 12:00 - 0903 18:00	1006
13	0930 12:00 - 1002 16:30	974	0901 12:00 - 0911 18:00	962
14	1003 01:00 - 1008 01:30	949	0905 18:00 - 0912 18:00	979
15	1006 03:30 - 1008 15:30	988	0906 6:00 - 0921 00:00	976
16	1008 22:30 - 1017 15:00	949	0917 12:00 - 0924 06:00	985
17	1018 05:30 - 1025 02:00	942	0918 00:00 - 0926 06:00	895
18	-	-	1001 12:00 - 1005 6:00	977
19	-	-	1005 06:00 - 1007 00:00	1001
20	-	-	1008 06:00 - 1011 12:00	988
21	-	-	1015 18:00 - 1026 18:00	882
22	-	-	1022 12:00 - 1024 18:00	998
23	-	-	1026 18:00 - 1031 00:00	962
24	-	-	1114 00:00 - 1122 00:00	1002
25	-	-	1119 12:00 - 1129 18:00	980
26	-	-	1129 06:00 - 1209 18:00	981
27	-	-	1230 00:00 - 0107 18:00	994

TABLE 1. Simulated (NR) and observed (BT) TCs, 2005 Atlantic Season.

ATLANTIC OCEAN 2006				
NATURE RUN			BEST TRACK	
TC No.	Start - end date (mmdd hh:hh)	Min SLP (hPa)	Start - end date (mmdd hh:hh)	Min SLP (hPa)
1	0818 10:00 - 0830 15:00	944	0610 06:00 - 0618 00:00	969
2	0902 00:00 - 0904 10:30	964	0718 12:00 - 0722 12:00	1000
3	0904 23:00 - 0908 23:30	962	0801 00:00 - 0806 12:00	1001
4	0907 13:00 - 0912 03:30	936	0821 18:00 - 0828 00:00	999
5	0912 15:30 - 0927 12:00	922	0824 18:00 - 0904 06:00	985
6	0917 03:00 - 0920 16:30	934	0903 18:00 - 0916 12:00	963
7	0921 19:00 - 0928 14:00	946	0910 18:00 - 0922 00:00	955
8	0929 04:30 - 1001 17:00	941	0912 12:00 - 0927 12:00	955
9	1006 21:00 - 1009 09:00	971	0927 18:00 - 1003 12:00	985
10	-	-	1103 11:00 - 1108 23:00	948

TABLE 2. Simulated (NR) and observed (BT) TCs, 2006 Atlantic Season.

EAST PACIFIC OCEAN 2005				
NATURE RUN			BEST TRACK	
TC No.	Start - end date (mmdd hh:hh)	Min SLP (hPa)	Start - end date (mmdd hh:hh)	Min SLP (hPa)
1	0729 17:30 - 0804 05:00	975	0517 18:00 - 0521 00:00	982
2	0802 20:30 - 0808 03:30	968	0621 18:00 - 0626 06:00	1000
3	0811 10:00 - 0813 22:30	967	0626 06:00 - 0703 12:00	1000
4	0909 08:00 - 0912 07:00	967	0704 00:00 - 0706 18:00	1002
5	0916 03:00 - 0903 22:00	962	0718 06:00 - 0721 18:00	989
6	0920 07:00 - 0922 13:00	968	0809 12:00 - 0817 12:00	978
7	1007 21:30 - 1010 22:30	968	0811 06:00 - 0815 18:00	1000
8	1022 13:00 - 1025 06:00	958	0819 18:00 - 0828 00:00	970
9	-	-	0825 12:00 - 0902 18:00	1000
10	-	-	0912 00:00 - 0925 00:00	951
11	-	-	0914 18:00 - 0930 18:00	947
12	-	-	0917 12:00 - 0919 00:00	1005
13	-	-	0917 12:00 - 0922 12:00	987
14	-	-	0923 00:00 - 1001 00:00	997
15	-	-	0928 00:00 - 1005 12:00	970

TABLE 3. Simulated (NR) and observed (BT) TCs, 2005 East Pacific Season.

EAST PACIFIC OCEAN 2006				
NATURE RUN			BEST TRACK	
TC No.	Start - end date (mmdd hh:hh)	Min SLP (hPa)	Start - end date (mmdd hh:hh)	Min SLP (hPa)
1	0531 05:30 - 0605 11:00	956	0527 06:00 - 0531 00:00	1002
2	0629 16:00 - 0706 11:30	969	0711 00:00 - 0717 12:00	953
3	0706 16:30 - 0715 02:30	948	0712 00:00 - 0720 00:00	981
4	0714 17:30 - 0719 15:00	966	0716 18:00 - 0728 12:00	933
5	0719 22:00 - 0722 06:30	964	0721 12:00 - 0731 12:00	990
6	0721 09:00 - 0726 18:00	955	0731 18:00 - 0805 18:00	1000
7	0727 09:00 - 0803 18:30	945	0801 00:00 - 0805 00:00	1004
8	0811 08:30 - 0814 06:30	955	0815 18:00 - 0824 06:00	966
9	0812 21:00 - 0815 16:30	970	0821 12:00 - 0829 06:00	955
10	0818 02:30 - 0820 19:30	972	0828 00:00 - 0904 12:00	948
11	0820 00:30 - 0822 09:00	972	0830 00:00 - 0909 06:00	985
12	0902 03:00 - 0912 18:30	935	0913 18:00 - 0917 12:00	952
13	0903 14:30 - 0910 16:00	939	0916 00:00 - 0921 06:00	999
14	0930 14:30 - 1007 03:00	946	1009 00:00 - 1015 18:00	1000
15	1006 09:30 - 1014 22:00	937	1009 18:00 - 1014 18:00	1000
16	1013 09:00 - 1017 01:00	940	1021 06:00 - 1026 06:00	970
17	1020 00:30 - 1022 13:00	988	1108 06:00 - 1110 18:00	1002
18	1022 13:00 - 1025 05:00	976	1113 18:00 - 1120 18:00	965
19	1120 16:30 - 1125 12:30	945	-	-

TABLE 4. Simulated (NR) and observed (BT) TCs, 2006 East Pacific Season.

NORTH WEST PACIFIC OCEAN 2005				
NATURE RUN			BEST TRACK	
TC No.	Start - end date (mmdd hh:hh)	Min SLP (hPa)	Start - end date (mmdd hh:hh)	Min SLP (hPa)
1	0701 05:00 - 0705 11:30	970	0113 00:00 - 0118 18:00	976
2	0705 14:00 - 0708 21:30	983	0312 00:00 - 0317 18:00	963
3	0712 05:30 - 0720 06:30	917	0416 18:00 - 0427 00:00	927
4	0802 21:00 - 0816 08:00	932	0527 12:00 - 0611 00:00	916
5	0803 21:30 - 0806 22:00	981	0710 12:00 - 0719 12:00	898
6	0813 16:00 - 0816 00:30	955	0718 00:00 - 0723 18:00	984
7	0816 18:00 - 0819 15:00	951	0721 12:00 - 0728 00:00	980
8	0817 10:00 - 0825 09:30	937	0728 18:00 - 0731 12:00	991
9	0824 19:00 - 0830 04:30	949	0729 18:00 - 0806 18:00	954
10	0830 16:30 - 0904 08:00	929	0809 18:00 - 0814 00:00	976
11	0901 07:30 - 0903 08:00	996	0818 00:00 - 0827 00:00	916
12	0905 16:00 - 0908 14:00	958	0817 06:00 - 0825 00:00	976
13	0905 18:30 - 0911 11:00	952	0824 18:00 - 0901 18:00	910
14	0906 02:30 - 0911 07:30	947	0828 18:00 - 0907 00:00	898
15	0909 19:30 - 0919 13:30	938	0905 06:00 - 0911 18:00	927
16	0921 16:30 - 0925 10:00	952	0914 06:00 - 0918 12:00	987
17	0926 04:00 - 0929 12:30	960	0920 06:00 - 0927 17:00	954
18	1001 19:00 - 1006 06:00	973	0919 00:00 - 0926 00:00	944
19	1005 12:30 - 1011 10:00	924	0925 00:00 - 1006 18:00	916
20	1007 08:00 - 1012 01:30	924	1006 06:00 - 1008 06:00	1000
21	1009 10:00 - 1016 20:00	930	1010 00:00 - 1019 00:00	927
22	1011 19:00 - 1020 07:30	927	1027 18:00 - 1102 12:00	958
23	1022 01:30 - 1028 02:00	953	1106 12:00 - 1112 12:00	991
24	-	-	1112 00:00 - 1120 18:00	972
25	-	-	1215 12:00 - 1221 06:00	991

TABLE 5. Simulated (NR) and observed (BT) TCs, 2005 North West Pacific Season.

NORTH WEST PACIFIC OCEAN				
NATURE RUN 2006			BEST TRACK 2006	
TC No.	Start - end date (mmdd hh:hh)	Min SLP (hPa)	Start - end date (mmdd hh:hh)	Min SLP (hPa)
1	0504 11:00 - 0514 14:00	932	0301 06:00 - 0307 00:00	997
2	0702 16:30 - 0705 16:30	958	0507 18:00 - 0519 00:00	916
3	0725 05:00 - 0803 08:30	906	0622 18:00 - 0629 06:00	991
4	0728 12:30 - 0731 16:00	961	0629 12:00 - 0710 12:00	910
5	0801 00:00 - 0802 02:00	941	0707 00:00 - 0714 12:00	987
6	0809 03:30 - 0813 11:30	980	0717 00:00 - 0726 00:00	967
7	0819 04:30 - 0827 05:00	930	0728 00:00 - 0805 00:00	972
8	0820 23:30 - 0824 03:00	956	0803 18:00 - 0810 18:00	980
9	0822 19:00 - 0825 15:30	961	0804 00:00 - 0812 06:00	898
10	0828 15:30 - 0901 04:00	970	0805 00:00 - 0811 00:00	984
11	0901 07:00 - 0906 09:00	923	0812 06:00 - 0820 00:00	984
12	0908 16:30 - 0916 05:00	911	0813 06:00 - 0816 12:00	991
13	0923 12:30 - 1001 02:00	924	0822 00:00 - 0825 06:00	1002
14	0929 15:30 - 1006 19:30	939	0909 00:00 - 0917 18:00	922
15	1006 05:00 - 1014 19:00	930	0912 00:00 - 0913 12:00	1000
16	1008 20:00 - 1016 09:00	962	0916 00:00 - 0925 06:00	898
17	1017 17:00 - 1023 23:00	946	0921 06:00 - 0925 00:00	1000
18	1107 01:00 - 1115 19:00	959	0925 06:00 - 1002 00:00	916
19	1108 08:30 - 1118 19:30	947	1003 06:00 - 1006 06:00	997
20	1123 19:30 - 1129 08:30	977	1003 00:00 - 1006 06:00	998
21	1127 10:30 - 1129 13:30	958	1008 12:00 - 1016 12:00	954
22	-	-	1025 00:00 - 1107 12:00	898
23	-	-	1107 06:00 - 1115 00:00	916
24	-	-	1124 12:00 - 1206 06:00	904
25	-	-	1206 00:00 - 1215 00:00	944
26	-	-	1215 18:00 - 1218 18:00	1000

TABLE 6. Simulated (NR) and observed (BT) TCs, 2006 North West Pacific Season.

NORTH INDIAN OCEAN				
NATURE RUN 2005			BEST TRACK 2005	
TC No.	Start - end date (mmdd hh:hh)	Min SLP (hPa)	Start - end date (mmdd hh:hh)	Min SLP (hPa)
1	1002 20:30 - 1005 01:30	962	0107 00:00 - 0110 12:00	1000
2	1119 06:00 - 1125 19:00	952	0111 18:00 - 0117 06:00	997
3	1204 18:30 - 1207 18:30	982	1001 06:00 - 1003 06:00	994
4	1212 16:30 - 1218 22:30	963	1025 00:00 - 1029 00:00	997
5	-	-	1126 06:00 - 1204 00:00	991
6	-	-	1204 06:00 - 1212 18:00	980
7	-	-	1214 18:00 - 1224 00:00	991
NATURE RUN 2006			BEST TRACK 2006	
1	0311 20:00 - 0315 08:30	966	0112 00:00 - 0119 06:00	991
2	0320 17:30 - 0325 10:30	970	0424 06:00 - 0429 12:00	922
3	1010 01:30 - 1015 02:30	981	0630 18:00 - 0703 12:00	997
4	1105 22:00 - 1109 04:30	952	0919 06:00 - 0926 12:00	984
5	1111 16:00 - 1116 04:30	952	0928 00:00 - 0930 00:00	997
6	1205 02:30 - 1208 02:30	971	1027 06:00 - 1030 12:00	984
7	-	-	1204 12:00 - 1209 18:00	976

TABLE 7. Simulated (NR) and observed (BT) TCs, North Indian Ocean Seasons: 2005 (above) and 2006 (below) .

SOUTH INDIAN OCEAN				
NATURE RUN 2005-06			BEST TRACK 2005-06	
TC No.	Start - end date (yyyy/mm/dd hh:hh)	Min SLP (hPa)	Start - end date (yyyy/mm/dd hh:hh)	Min SLP (hPa)
1	2005/10/19 02:00 - 2005/10/21 05:00	981	2005/10/13 18:00 - 2005/10/17 06:00	994
2	2005/10/30 18:30 - 2005/11/02 18:00	966	2005/11/04 06:00 - 2005/11/08 06:00	997
3	2005/11/02 07:00 - 2005/11/05 22:30	972	2005/11/18 06:00 - 2005/11/29 06:00	927
4	2005/11/15 15:30 - 2005/11/21 15:00	945	2005/12/17 00:00 - 2005/12/29 18:00	997
5	2005/12/01 15:00 - 2005/12/06 23:00	958	2006/01/22 12:00 - 2006/02/06 06:00	944
6	2006/01/12 12:00 - 2006/01/14 13:30	969	2006/02/18 00:00 - 2006/02/23 18:00	991
7	2006/01/14 19:00 - 2006/01/21 10:00	931	2006/02/22 12:00 - 2006/03/02 18:00	910
8	2006/01/15 13:30 - 2006/01/22 04:00	939	2006/03/01 06:00 - 2006/03/09 06:00	984
9	2006/01/26 10:00 - 2006/02/03 02:30	944	2006/04/03 12:00 - 2006/04/16 12:00	985
10	2006/02/05 22:00 - 2006/02/14 00:00	949	-	-
11	2006/02/12 18:00 - 2006/02/21 16:00	937	-	-
12	2006/02/13 20:30 - 2006/02/22 08:00	916	-	
13	2006/02/28 12:00 - 2006/03/04 14:30	930	-	
14	2006/03/04 03:30 - 2006/03/12 17:00	923	-	
15	2006/03/14 01:30 - 2006/03/18 23:30	955	-	
16	2006/03/20 10:30 - 2006/03/22 19:00	972	-	
17	2006/03/24 16:30 - 2006/03/27 12:00	982	-	
18	2006/04/03 08:30 - 2006/04/06 23:00	954	-	

TABLE 8. Simulated (NR) and observed (BT) TCs, 2005-2006 South Indian Ocean Season.

SOUTH INDIAN OCEAN				
NATURE RUN 2006-07			BEST TRACK 2006-07	
TC No.	Start - end date (yyyy/mm/dd hh:hh)	Min SLP (hPa)	Start - end date (yyyy/mm/dd hh:hh)	Min SLP (hPa)
1	2006/11/21 07:00 - 2006/11/25 03:30	973	2006/11/27 06:00 - 2006/12/04 00:00	989
2	2006/12/20 00:30 - 2006/12/24 17:00	934	2006/12/16 00:00 - 2006/12/26 18:00	904
3	2006/12/28 04:00 - 2006/12/30 16:00	980	2006/12/29 12:00 - 2007/01/04 18:00	976
4	2007/01/10 10:00 - 2007/01/16 20:00	933	2006/01/28 06:00 - 2007/02/10 00:00	927
5	2007/01/15 19:30 - 2007/01/25 20:30	919	2007/02/05 18:00 - 2007/02/12 00:00	981
6	2007/01/24 17:00 - 2007/01/31 12:00	938	2007/02/11 18:00 - 2007/02/23 12:00	922
7	2007/02/03 14:00 - 2007/02/09 01:00	924	2007/02/19 06:00 - 2007/03/03 00:00	938
8	2007/02/14 23:30 - 2007/02/24 01:00	940	2007/02/20 18:00 - 2007/03/01 06:00	963
9	2007/02/15 18:30 - 2007/02/27 00:00	914	2007/03/07 00:00 - 2007/03/17 06:00	927
10	2007/03/06 18:00 - 2007/03/14 16:30	949	-	-
11	2007/03/07 18:30 - 2007/03/12 01:00	959	-	-
12	2007/03/15 01:00 - 2007/03/19 12:00	965	-	-

TABLE 9. Simulated (NR) and observed (BT) TCs, 2006-2007 South Indian Ocean Season.

AUSTRALIAN REGION 2005-2006				
NATURE RUN			BEST TRACK	
TC No.	Start - end date (yyyy/mm/dd hh)	Min SLP (hPa)	Start - end date (yyyy/mm/dd hh)	Min SLP (hPa)
1	2005/11/12 16:00 - 2005/11/15 15:30	975	2006/01/06 18:00 - 2006/01/10 18:00	980
2	2005/11/22 19:00 - 2005/11/29 06:00	959	2006/01/11 06:00 - 2006/01/14 06:00	994
3	2005/11/26 14:00 - 2005/11/29 06:30	968	2006/01/13 12:00 - 2006/01/15 06:00	980
4	2005/12/18 18:00 - 2005/12/22 00:00	982	2006/01/18 12:00 - 2006/01/23 12:00	987
5	2005/12/22 08:00 - 2005/12/31 19:30	975	2006/01/27 00:00 - 2006/02/02 18:00	963
6	2005/12/26 15:30 - 2005/12/31 17:00	975	2006/02/10 18:00 - 2006/02/17 18:00	967
7	2006/01/04 07:00 - 2006/01/07 02:00	984	2006/02/22 06:00 - 2006/02/24 00:00	989
8	2006/01/07 15:00 - 2006/01/09 21:00	986	2006/02/26 18:00 - 2006/02/28 12:00	997
9	2006/01/08 12:30 - 2006/01/21 19:30	949	2006/03/16 12:00 - 2006/03/21 06:00	937
10	2006/01/18 10:00 - 2006/01/23 07:30	987	2006/03/18 00:00 - 2006/03/25 06:00	963
11	2006/02/08 09:00 - 2006/02/11 15:00	980	2006/03/19 00:00 - 2006/03/27 00:00	927
12	2006/02/09 10:30 - 2006/02/15 11:00	938	2006/03/23 12:00 - 2006/03/31 00:00	922
13	2006/02/17 05:00 - 2006/02/23 01:30	937	2006/04/03 00:00 - 2006/04/08 06:00	984
14	2006/02/26 18:00 - 2006/03/01 06:30	935	2006/04/16 18:00 - 2006/04/26 18:00	879
15	2006/03/01 10:30 - 2006/03/07 08:00	985	-	-
16	2006/03/04 07:30 - 2006/03/06 21:30	961	-	-
17	2006/04/19 22:00 - 2006/04/29 17:00	905	-	-

TABLE 10. Simulated (NR) and observed (BT) TCs, 2005-2006 Australian Region Season.

AUSTRALIAN REGION 2006-2007				
NATURE RUN			BEST TRACK	
TC No.	Start - end date (yyyy/mm/dd hh:hh)	Min SLP (hPa)	Start - end date (yyyy/mm/dd hh:hh)	Min SLP (hPa)
1	2007/01/02 00:00 - 2007/01/06 03:00	932	2006/10/20 12:00 - 2006/10/26 06:00	927
2	2007/01/08 18:30 - 2007/01/10 20:30	985	2006/11/18 18:00 - 2006/11/27 00:00	972
3	2007/01/09 16:00 - 2007/01/18 09:30	941	2006/12/01 00:00 - 2006/12/03 00:00	997
4	2007/01/16 06:30 - 2007/01/24 21:00	949	2006/12/31 00:00 - 2007/01/03 06:00	994
5	2007/01/16 20:30 - 2007/01/24 10:00	940	2007/01/21 06:00 - 2007/01/24 12:00	980
6	2007/01/29 06:00 - 2007/02/06 23:30	940	2007/01/21 06:00 - 2007/01/27 06:00	974
7	2007/02/01 13:30 - 2007/02/07 04:30	920	2007/02/01 18:00 - 2007/02/05 18:00	997
8	2007/02/13 10:30 - 2007/02/15 15:00	983	2007/02/02 18:00 - 2007/02/07 06:00	987
9	2007/02/18 13:00 - 2007/02/21 19:30	970	2007/02/28 06:00 - 2007/03/10 00:00	941
10	2007/02/25 13:00 - 2007/03/01 09:30	941	2007/03/03 00:00 - 2007/03/12 18:00	967
11	2007/03/02 16:30 - 2007/03/07 17:30	981	2007/03/24 06:00 - 2007/03/29 06:00	944
12	2007/03/09 15:00 - 2007/03/11 23:00	960	2007/03/24 18:00 - 2007/03/29 18:00	970
13	2007/03/13 19:00 - 2007/03/21 04:00	941	2007/04/02 18:00 - 2007/04/06 18:00	982
14	2007/03/21 10:30 - 2007/03/29 21:00	927	2007/05/15 12:00 - 2007/05/23 00:00	1000
15	2007/04/06 01:00 - 2007/04/11 17:30	917	-	-
16	2007/04/26 19:30 - 2007/04/29 22:30	972	-	-
17	2007/05/03 00:30 - 2007/05/05 19:30	989	-	-

TABLE 11. Simulated (NR) and observed (BT) TCs, 2006-2007 Australian Region Season.

LIST OF FIGURES

Fig. 1. Vertical meridional cross section of zonal wind at 0^o longitude ($m s^{-1}$) in the G5NR (left) and MERRA-2 (right), for 2005 (above) and 2006 (below). 53

Fig. 2. African easterly wave activity in the G5NR (above) and in MERRA-2 (below): Hovmøller plots of meridional winds at about 700 hPa (level 55), August 2005. Time increasing upwards. 54

Fig. 3. Same as Fig 2, but for 2006. 55

Fig. 4. Simulated and observed 2005 Atlantic TCs from the G5NR (a) and the NHC best tracks (b). Individual cyclone track colors indicate center pressure from the 7 km output. Open circles are drawn at the beginning of tracks. Corresponding start and end dates are listed in Table 1. . 56

Fig. 5. As in Fig 4, but for 2006. Corresponding dates in Table 2. 57

Fig. 6. Structure of G5NR 2005 Atlantic TC no. 2, (see Fig 4 and Table 1). Zonal vertical cross-sections of winds (shaded, $m s^{-1}$) and temperature (black contours, ^oC). Temperature anomalies (^oC, red thick contours, contours every 2^oC, only values $> 8^oC$ are plotted for clarity), with respect to a zonal mean within 10^o of the TC center. Vertical coordinate in model levels. Levels 72, 50 and 40 correspond to nominal pressures of 985.00 hPa, 487.500 hPa and 127.837 hPa respectively, at the top edge of the layer. Full conversion table in da Silva et al. (2015). 58

Fig. 7. Structure of G5NR 2005 Atlantic TC no. 12, hereafter G5NR AL122005, during its mature phase. Above: as Fig. 6. Below: map of total wind (shaded, $m s^{-1}$) at maximum wind level (approx. 900 hPa) with superimposed 17 $m s^{-1}$, 25 $m s^{-1}$ and 32 $m s^{-1}$ isotachs (solid). . . . 59

Fig. 8. Sea level pressure and 10 m wind transects for G5NR AL122005, at the same time and latitude as in Fig. 7. Radii of wind at 17 $m s^{-1}$, 25 $m s^{-1}$ and 32 $m s^{-1}$ ($R17, R25, R32$) are shown with orange, red and magenta lines. 60

Fig. 9. Hourly accumulated precipitation ($mm m h^{-1}$) for G5NR 2006 Atlantic TC no. 4 (see Fig. 5 and Table 2), compared with NEXRAD level 3 accumulated hourly precipitation for Katrina at 12:30Z 29 August 2005. 61

Fig. 10. Simulated and observed 2005 eastern North Pacific TCs from the G5NR (a) and best tracks (b). Colors as in Fig 4. Corresponding dates in Table 3. 62

Fig. 11. As in Fig. 10, but for 2006. Corresponding dates in Table 4. 63

Fig. 12. Hovmøller of Equatorial low-level zonal wind in JJA 2006 across the central Pacific from the G5NR (left, at level 70) and from MERRA-2 (right, at 950 hPa). 64

Fig. 13. Simulated and observed 2005 western North Pacific TCs from the G5NR (a) and best tracks (b). Colors as in Fig 4. Corresponding dates in Table 5. 65

Fig. 14. As in Fig. 13, but for 2006. Corresponding dates in Table 6. Observed TC 24 (named Typhoon Dorian) will enter into the North Indian Ocean as TC no. 7. 66

Fig. 15. Structure of G5NR 2006 western North Pacific TC no. 3 (G5NR-WP032006) (Fig 14 and Table 6). As in Fig 6, except that both zonal and meridional vertical cross-sections are

plotted, and temperature anomalies are in grey thick contours (every 4^oC, only values $>$ 10^oC for clarity). 67

Fig. 16. Wind in July 2006 at 900 hPa across the Indian Ocean in the G5NR (above) and in MERRA-2 (below). 68

Fig. 17. Vertical meridional cross section of the Somali Jet in July 2006 and at longitude 55^oE in the G5NR (above) and in MERRA-2 (below). 69

Fig. 18. Simulated and observed 2005 North Indian Ocean TCs from the G5NR (a) and BT (b). Colors as in Fig. 4. Corresponding dates in Table 7. 70

Fig. 19. Simulated and observed 2006 North Indian Ocean TCs from the G5NR (a) and BT (b). Colors as in Fig. 4. Corresponding dates in Table 7. Observed data show Typhoon Dorian (renamed TC 7) crossing the Malay peninunsula from the Pacific and entering the Bay of Bengal as a tropical depression 71

Fig. 20. Simulated and observed 2005-2006 South Indian Ocean TCs from the G5NR (a) and BT (b). Colors as in Fig. 4. Corresponding dates in Table 8. 72

Fig. 21. Simulated and observed 2006-2007 South Indian Ocean TCs from the G5NR (a) and BT (b). Colors as in Fig. 4. Corresponding dates in Table 9. 73

Fig. 22. Structure of G5NR 2006-2007 South Indian Ocean TC no. 5 (Fig 21 and Table 9). As in Fig. 6, except that both zonal and meridional vertical cross-sections are plotted. 74

Fig. 23. Simulated and observed 2005-2006 Australian region TCs from the G5NR (a) and BT (b). Colors as in Fig. 4. Corresponding dates in Table 10. 75

Fig. 24. Simulated and observed 2006-2007 Australian region TCs from the G5NR (a) and BT (b). Colors as in Fig. 4. Corresponding dates in Table 11. 76

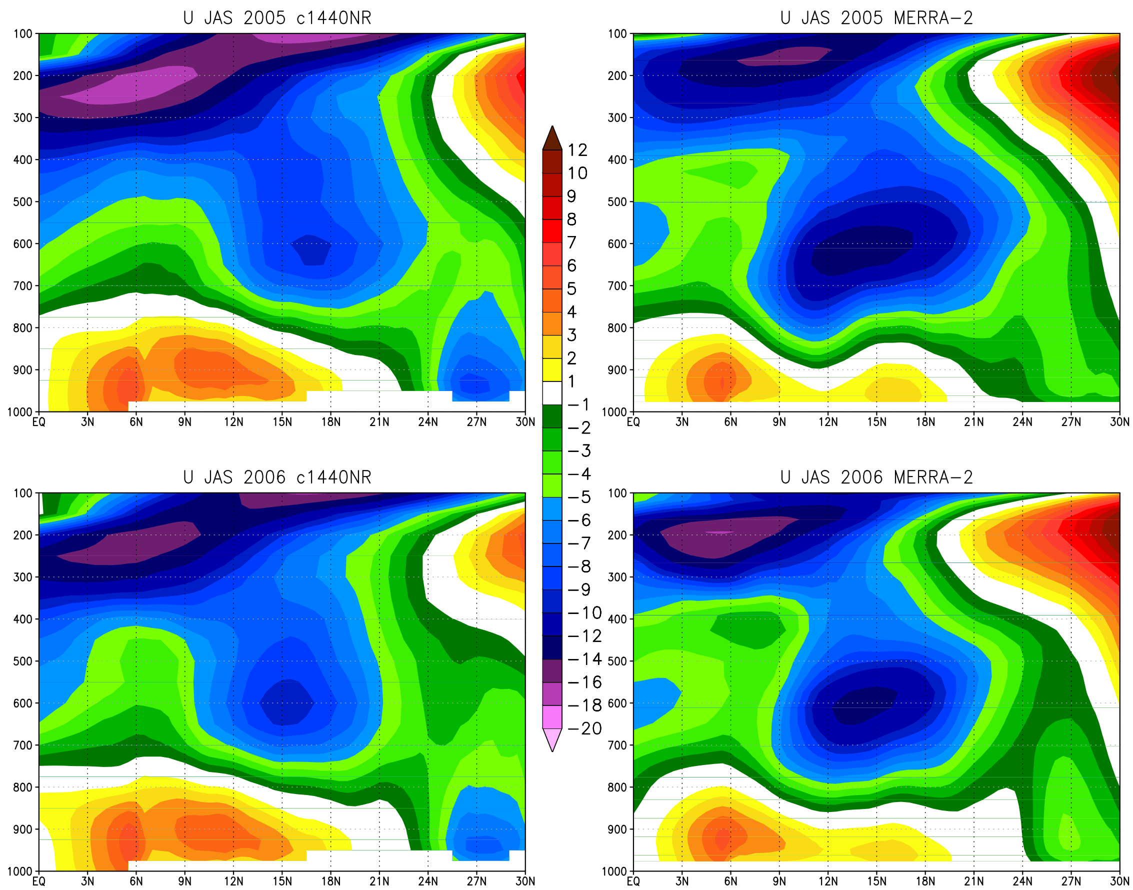

FIG. 1. Vertical meridional cross section of zonal wind at 0^o longitude ($m s^{-1}$) in the G5NR (left) and MERRA-2 (right), for 2005 (above) and 2006 (below).

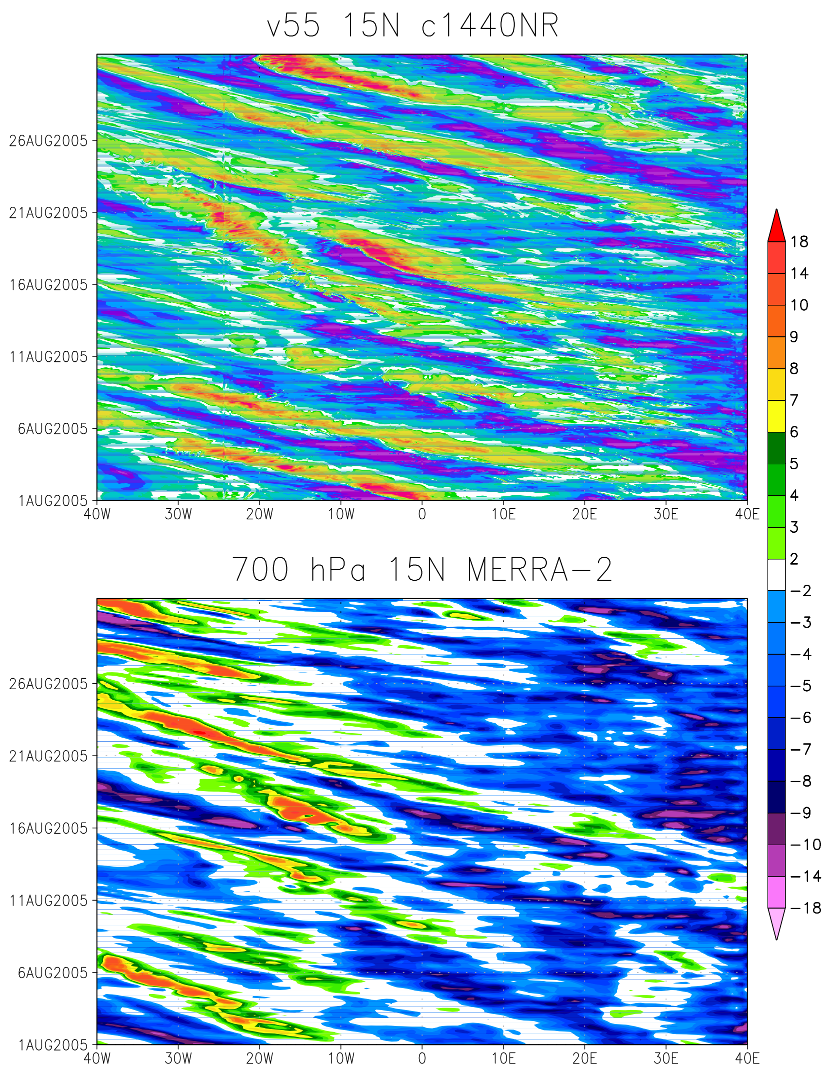

FIG. 2. African easterly wave activity in the G5NR (above) and in MERRA-2 (below): Hovmøller plots of meridional winds at about 700 hPa (level 55), August 2005. Time increasing upwards.

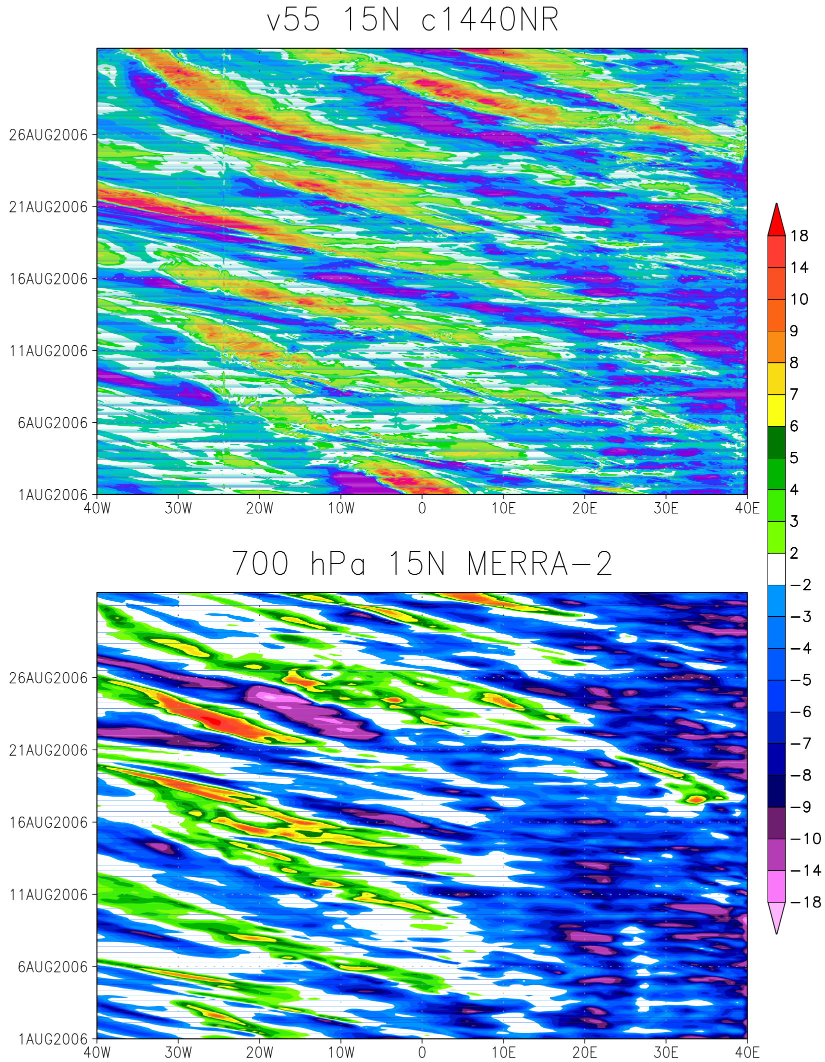

FIG. 3. Same as Fig 2, but for 2006.

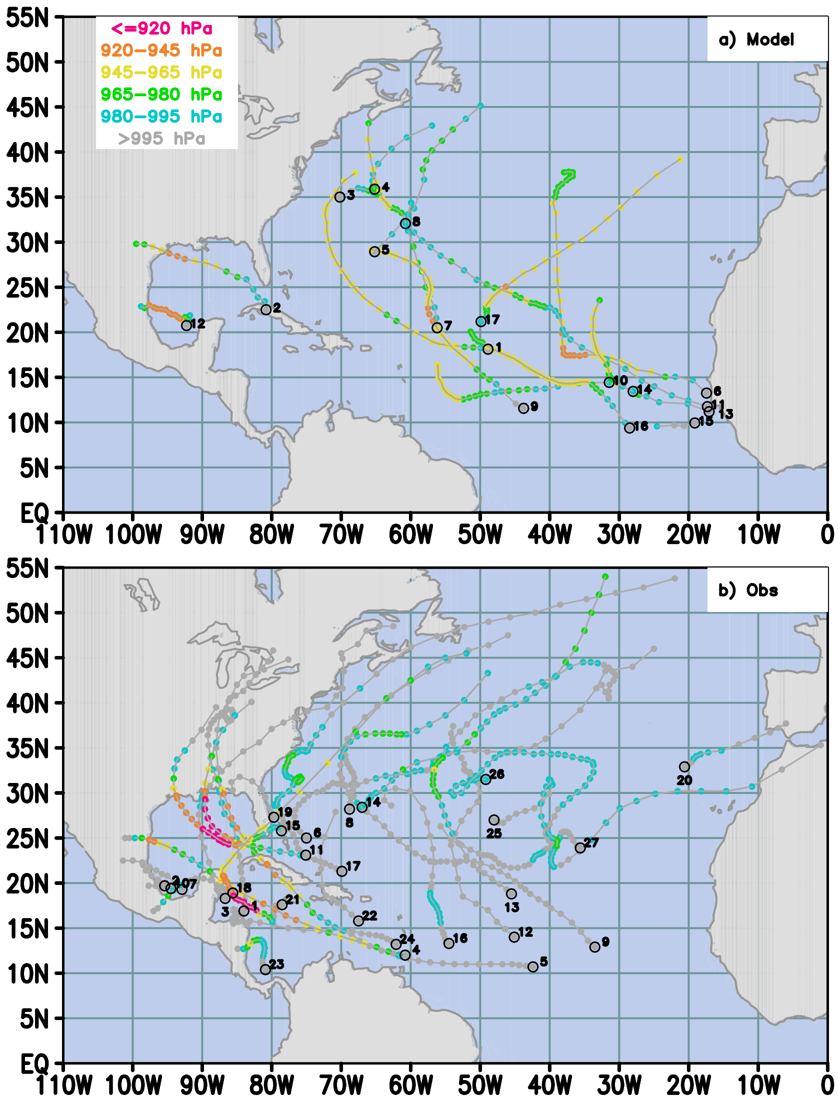

FIG. 4. Simulated and observed 2005 Atlantic TCs from the G5NR (a) and the NHC best tracks (b). Individual cyclone track colors indicate center pressure from the 7 km output. Open circles are drawn at the beginning of tracks. Corresponding start and end dates are listed in Table 1.

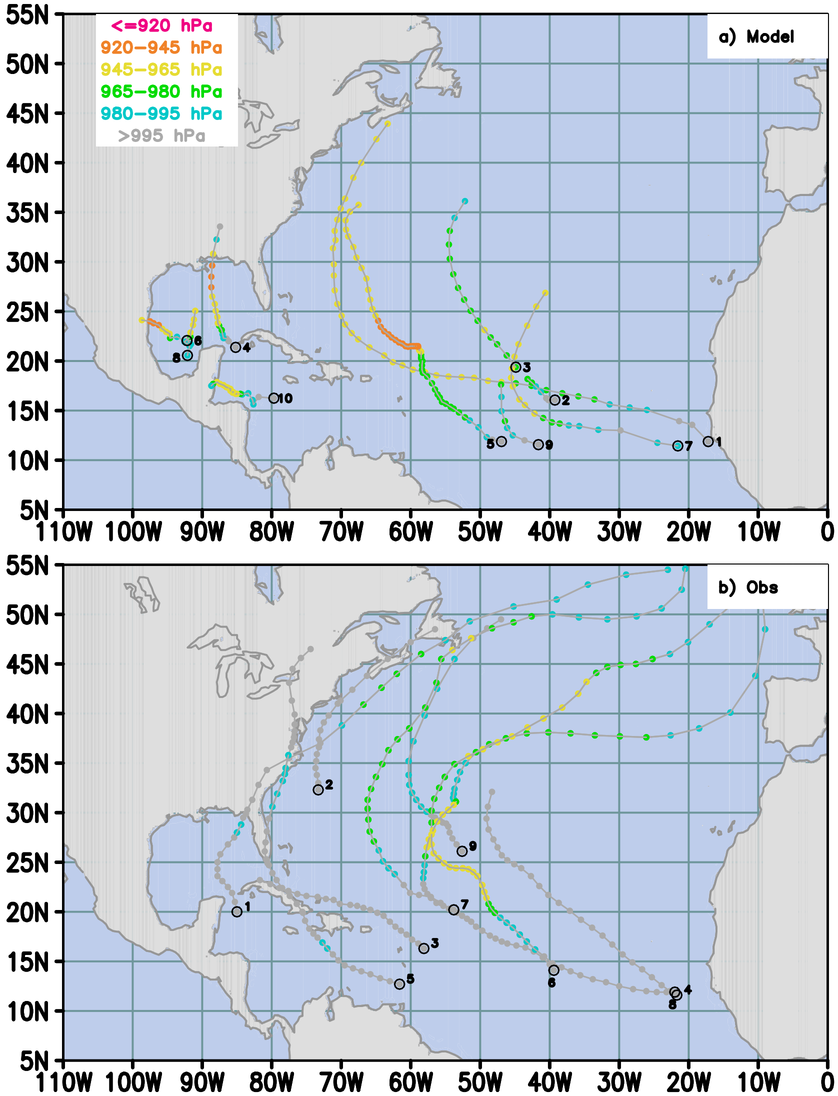

FIG. 5. As in Fig 4, but for 2006. Corresponding dates in Table 2.

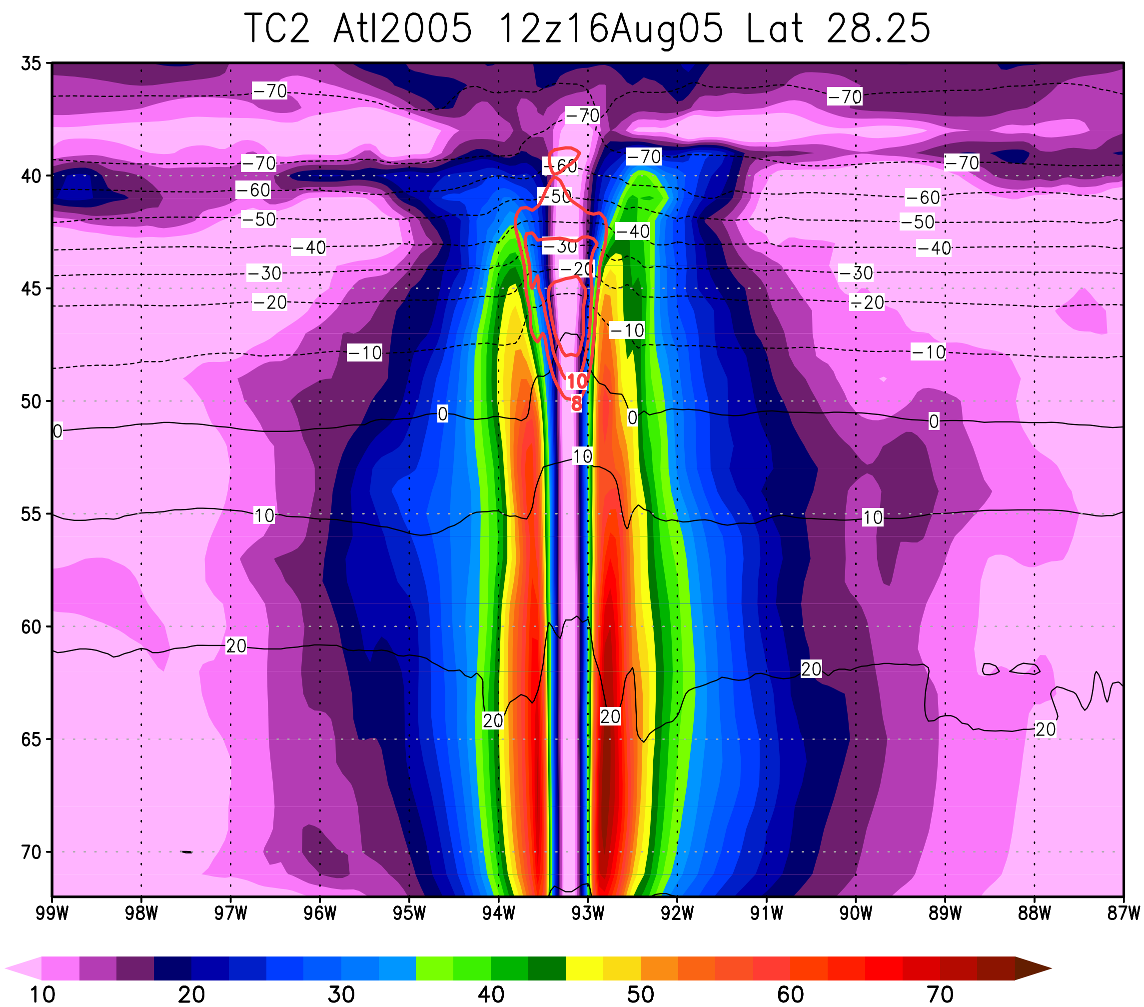

FIG. 6. Structure of G5NR 2005 Atlantic TC no. 2, (see Fig 4 and Table 1). Zonal vertical cross-sections of winds (shaded, $m s^{-1}$) and temperature (black contours, ^oC). Temperature anomalies (^oC, red thick contours, contours every 2^oC, only values $> 8^oC$ are plotted for clarity), with respect to a zonal mean within 10^o of the TC center. Vertical coordinate in model levels. Levels 72, 50 and 40 correspond to nominal pressures of 985.00 hPa, 487.500 hPa and 127.837 hPa respectively, at the top edge of the layer. Full conversion table in da Silva et al. (2015).

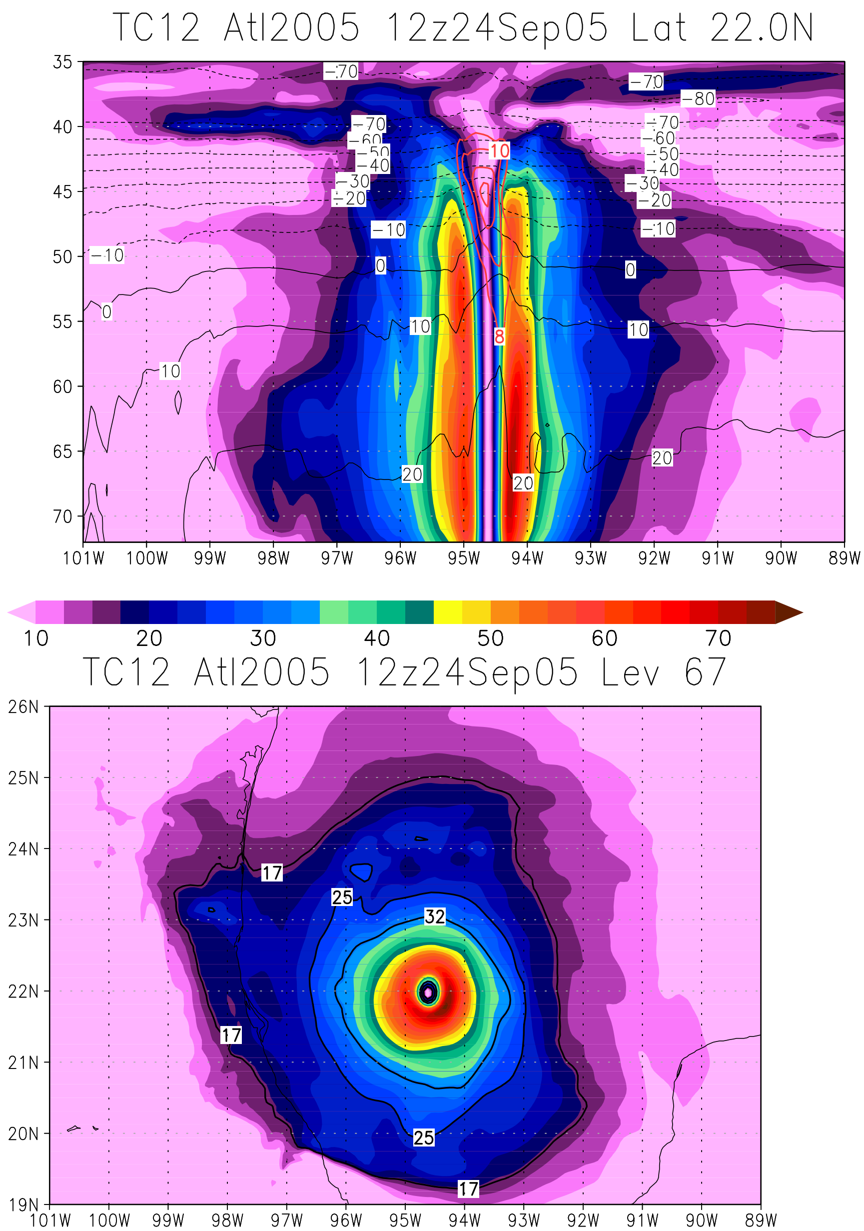

FIG. 7. Structure of G5NR 2005 Atlantic TC no. 12, hereafter G5NR AL122005, during its mature phase. Above: as Fig. 6. Below: map of total wind (shaded, $m s^{-1}$) at maximum wind level (approx. 900 hPa) with superimposed 17 $m s^{-1}$, 25 $m s^{-1}$ and 32 $m s^{-1}$ isotachs (solid).

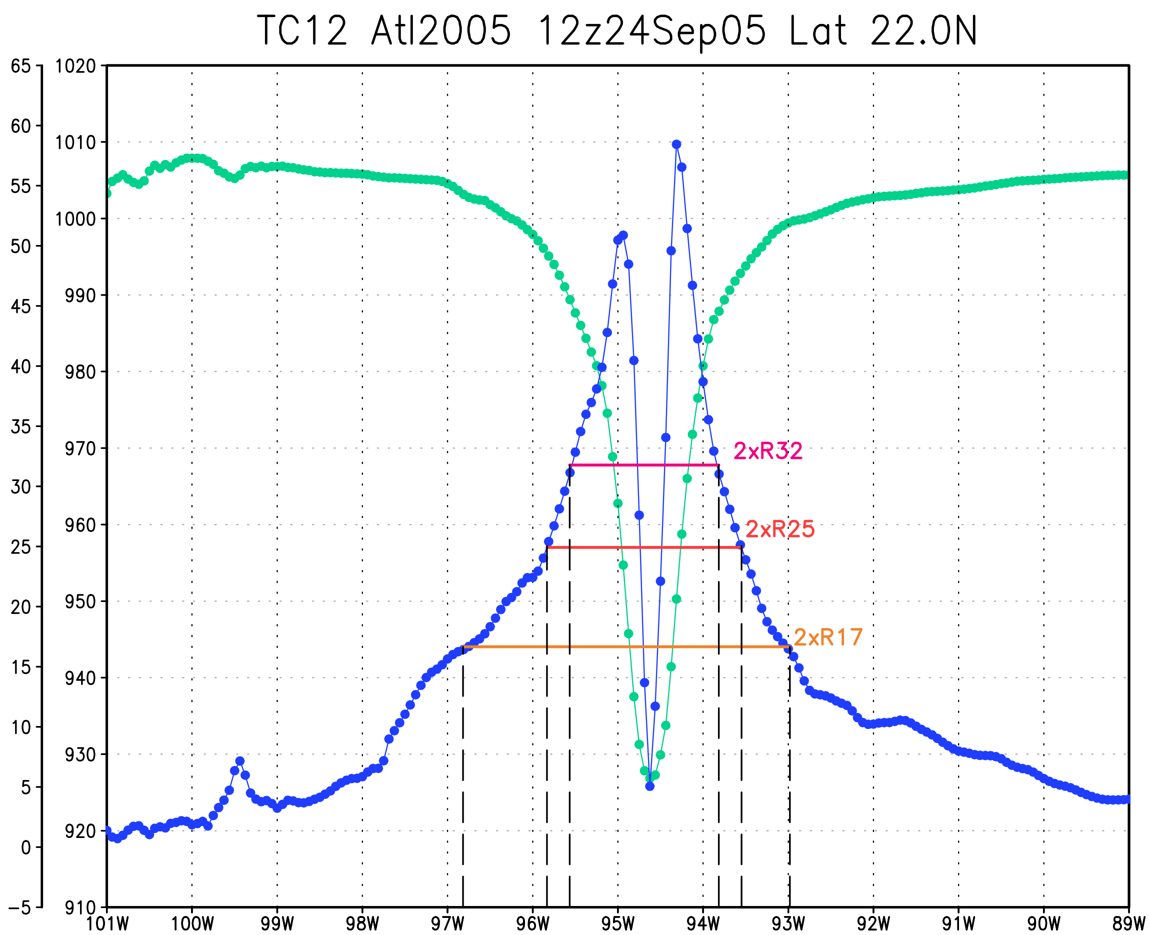

937 FIG. 8. Sea level pressure and 10 m wind transects for G5NR AL122005, at the same time and latitude as
938 in Fig. 7. Radii of wind at 17 ms^{-1}, 25 ms^{-1} and 32 ms^{-1} ($R17, R25, R32$) are shown with orange, red and
939 magenta lines.

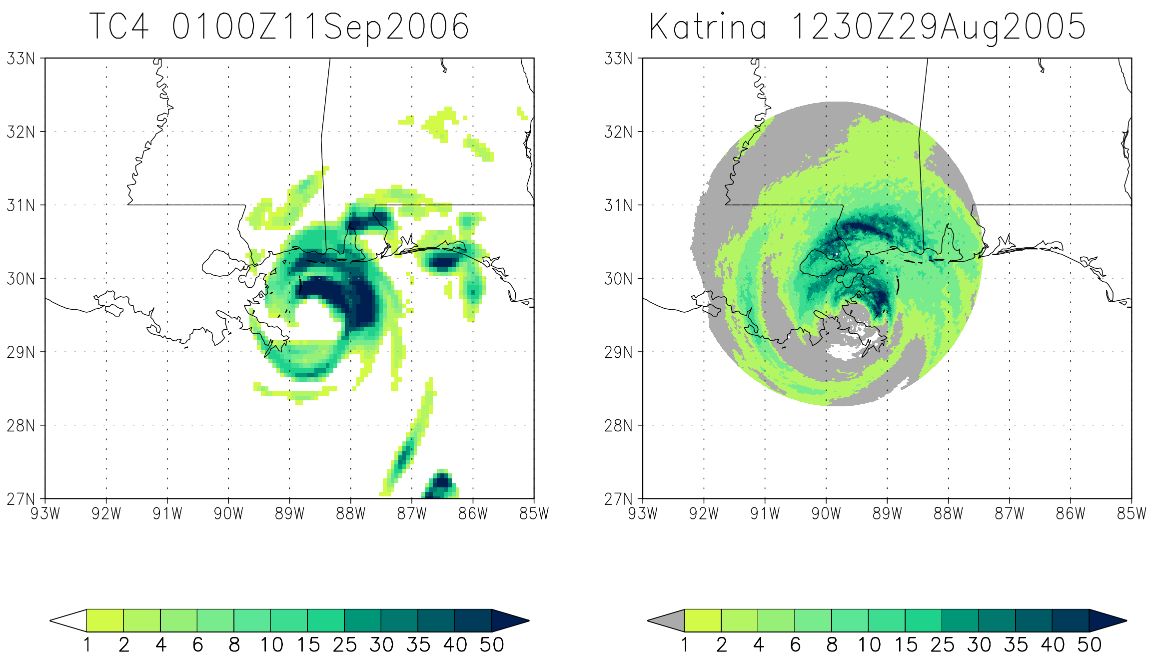

FIG. 9. Hourly accumulated precipitation ($mm\,h^{-1}$) for G5NR 2006 Atlantic TC no. 4 (see Fig. 5 and Table 2), compared with NEXRAD level 3 accumulated hourly precipitation for Katrina at 12:30Z 29 August 2005.

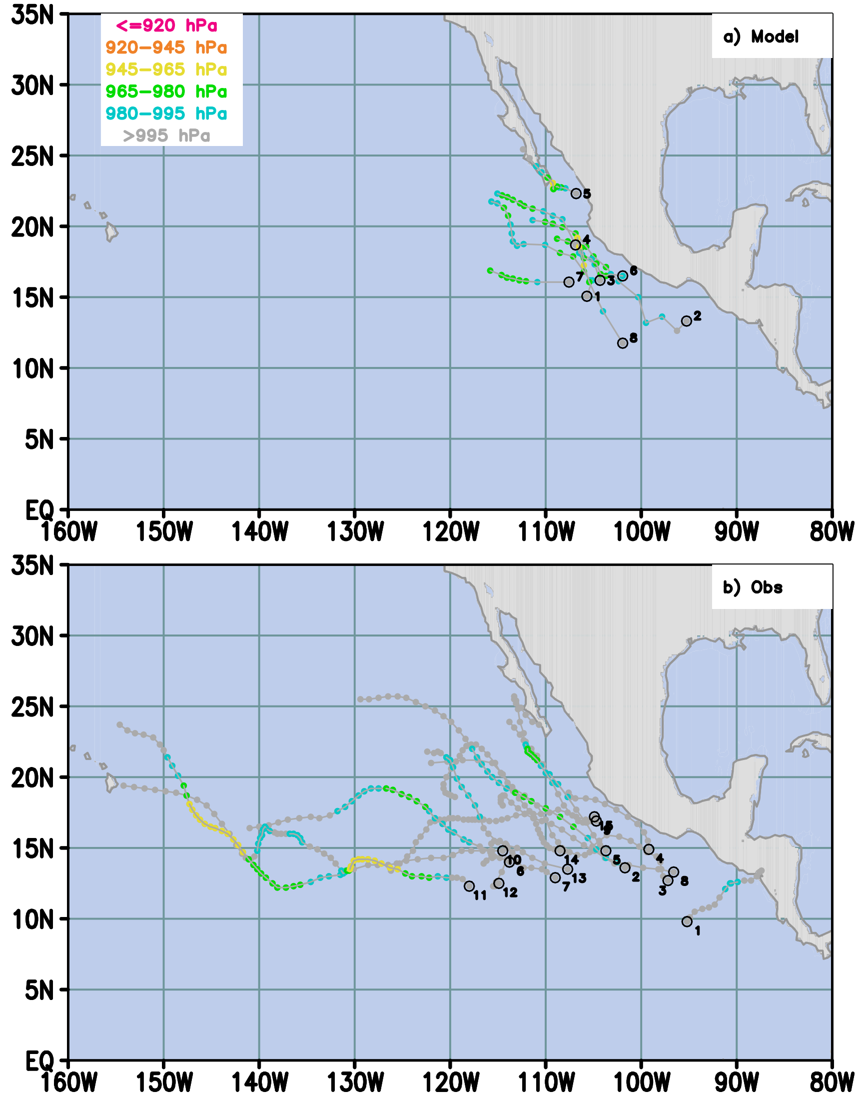

943 FIG. 10. Simulated and observed 2005 eastern North Pacific TCs from the G5NR (a) and best tracks (b).
944 Colors as in Fig 4. Corresponding dates in Table 3.

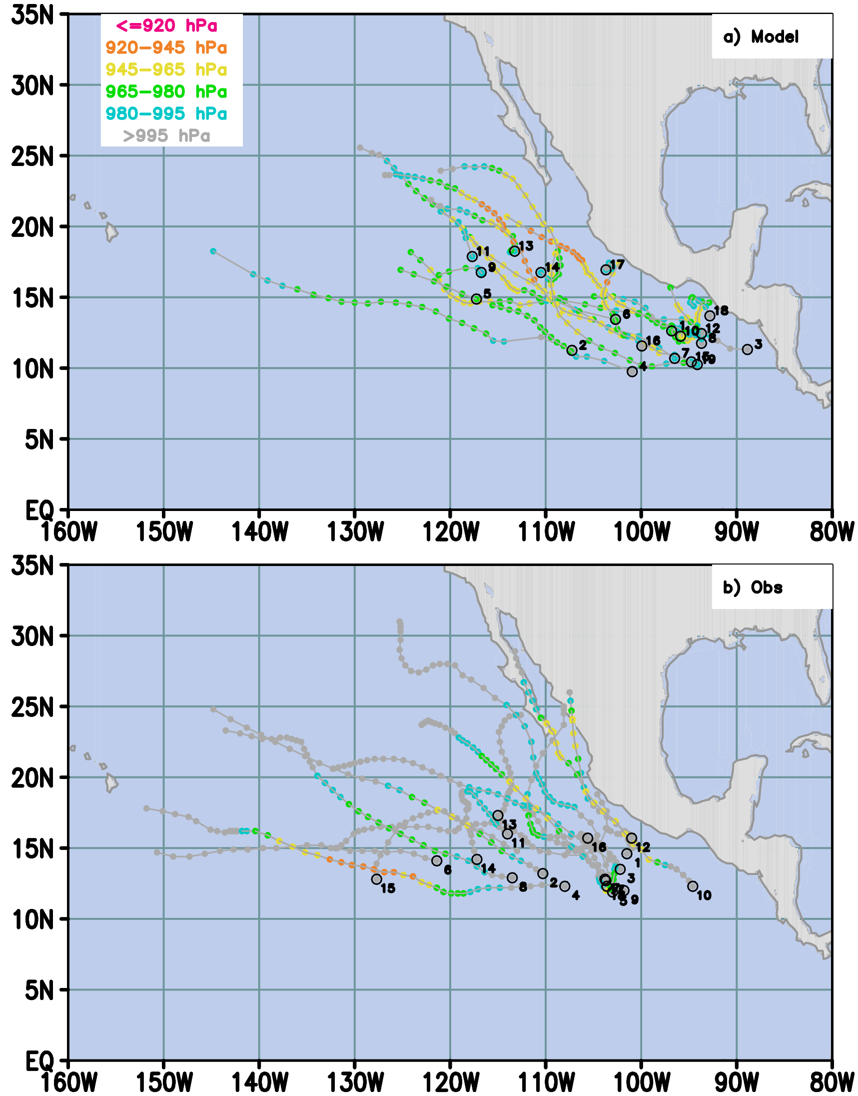

FIG. 11. As in Fig. 10, but for 2006. Corresponding dates in Table 4.

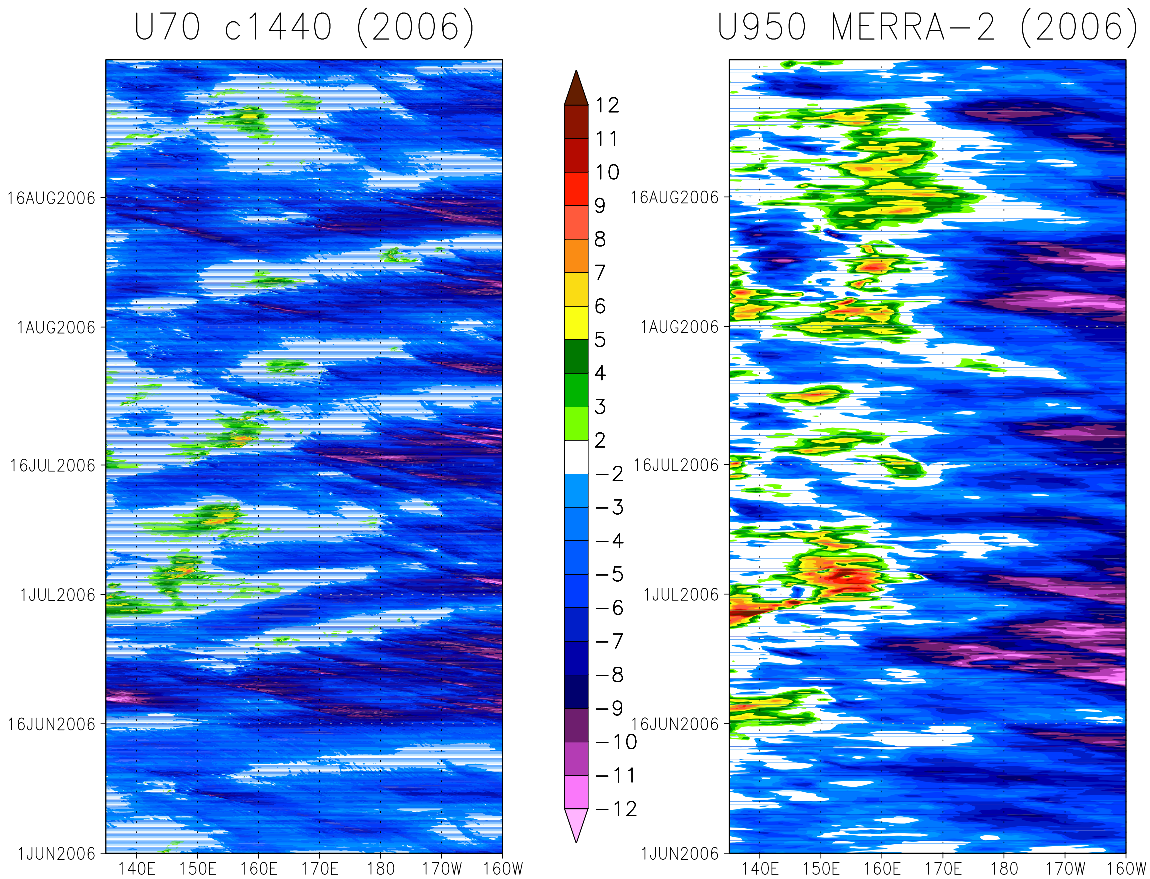

945 FIG. 12. Hovmøller of Equatorial low-level zonal wind in JJA 2006 across the central Pacific from the G5NR
946 (left, at level 70) and from MERRA-2 (right, at 950 hPa).

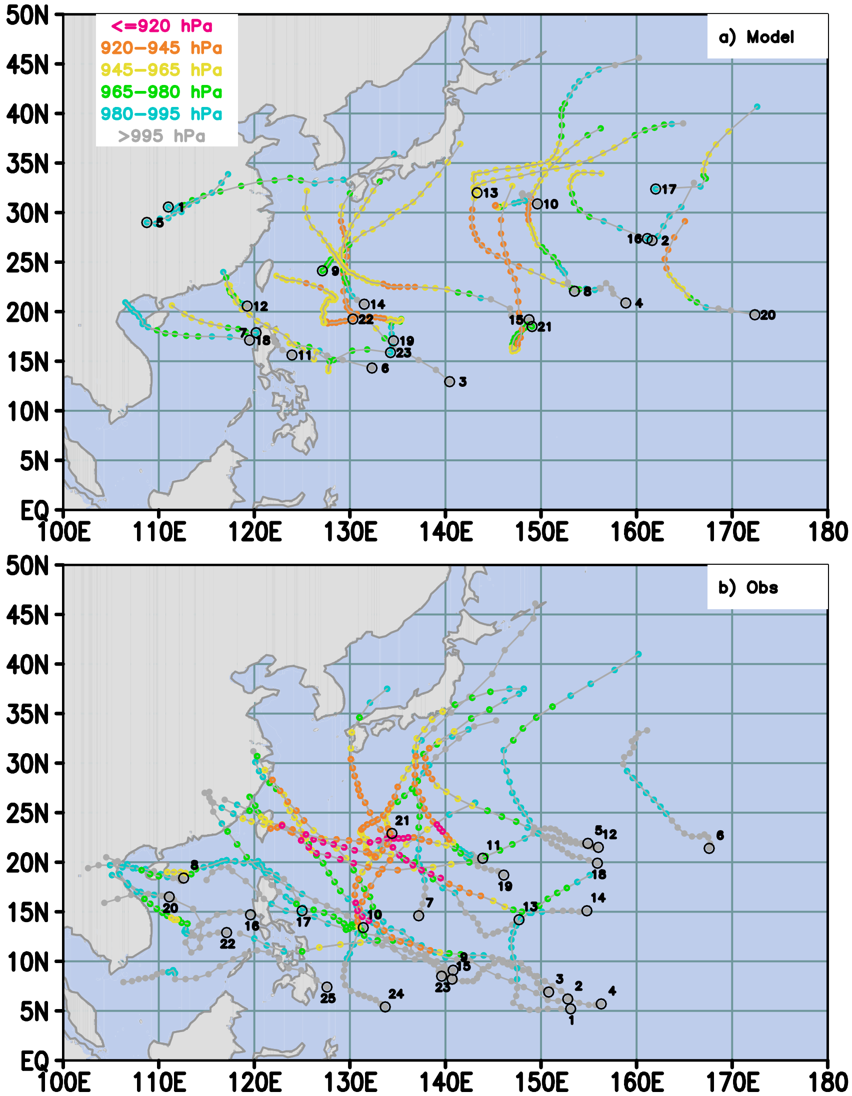

FIG. 13. Simulated and observed 2005 western North Pacific TCs from the G5NR (a) and best tracks (b). Colors as in Fig 4. Corresponding dates in Table 5.

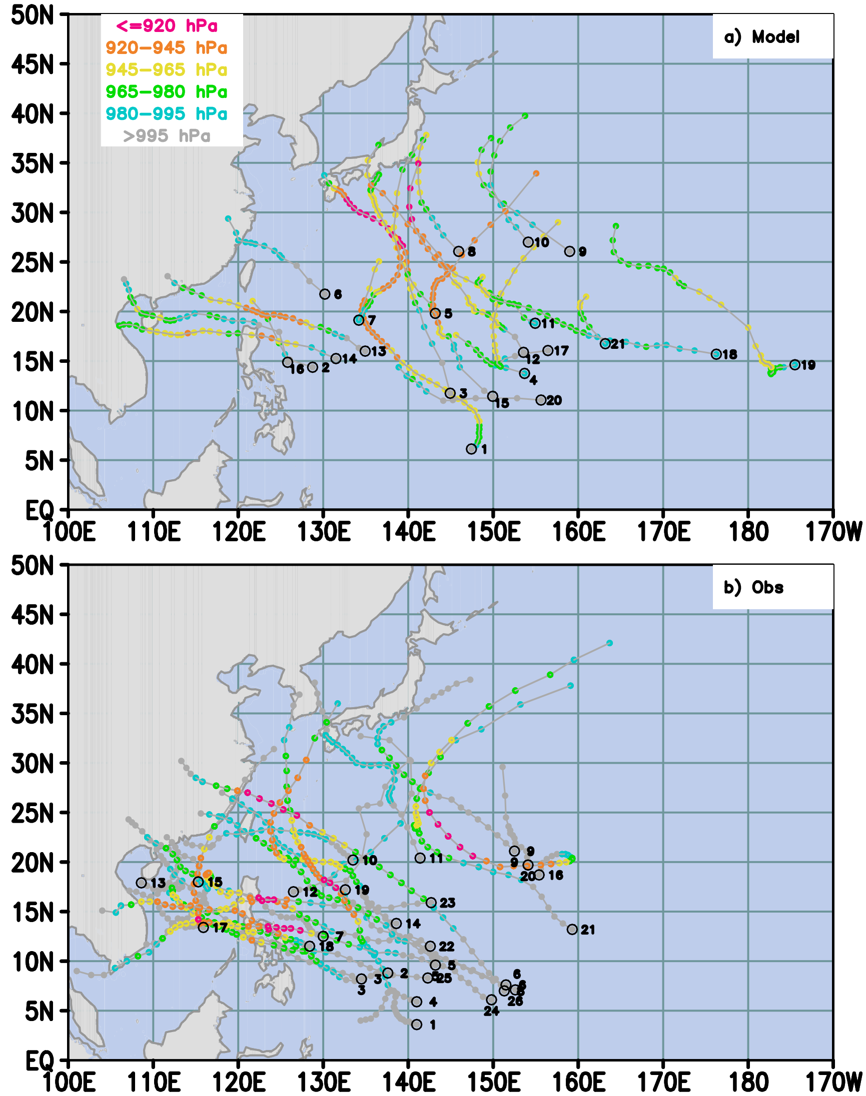

FIG. 14. As in Fig. 13, but for 2006. Corresponding dates in Table 6. Observed TC 24 (named Typhoon Dorian) will enter into the North Indian Ocean as TC no. 7.

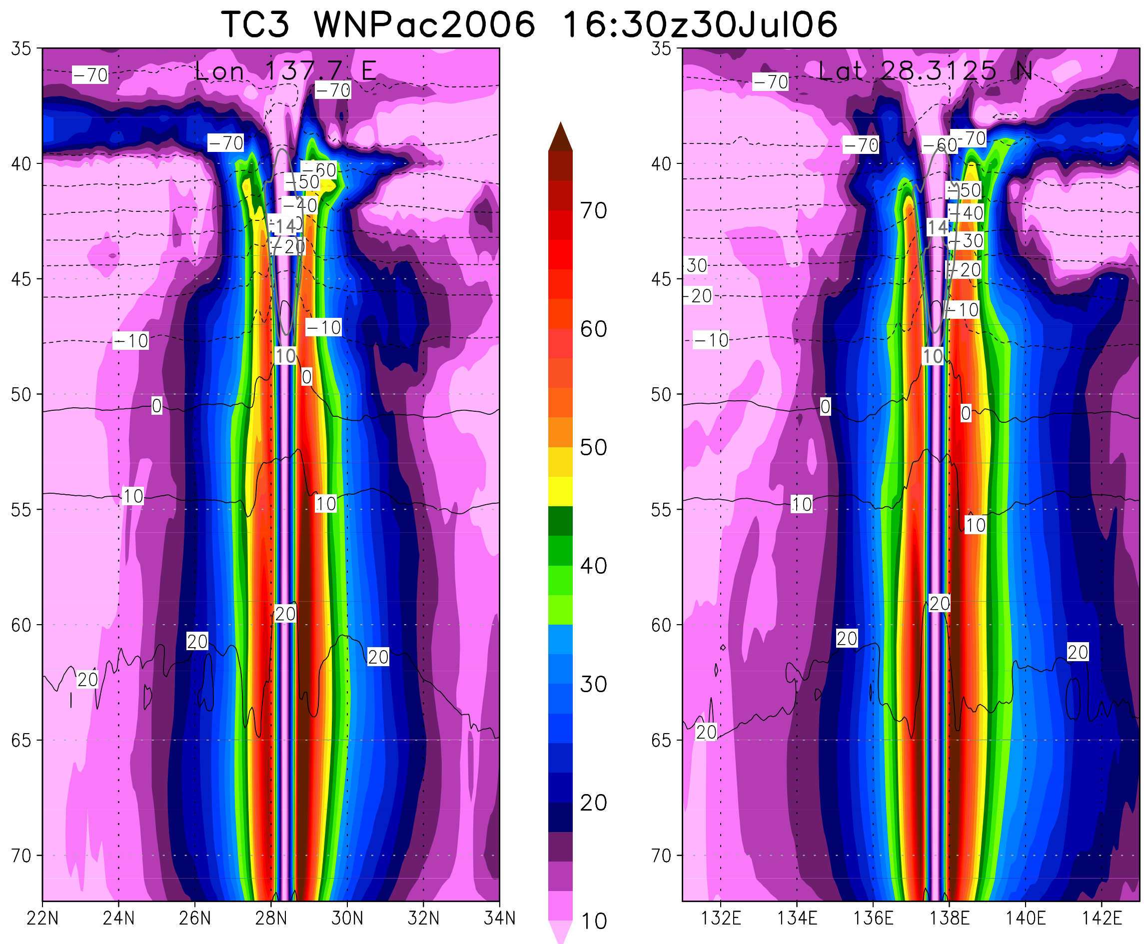

FIG. 15. Structure of G5NR 2006 western North Pacific TC no. 3 (G5NR-WP032006) (Fig 14 and Table 6). As in Fig 6, except that both zonal and meridional vertical cross-sections are plotted, and temperature anomalies are in grey thick contours (every 4^oC, only values $> 10^oC$ for clarity).

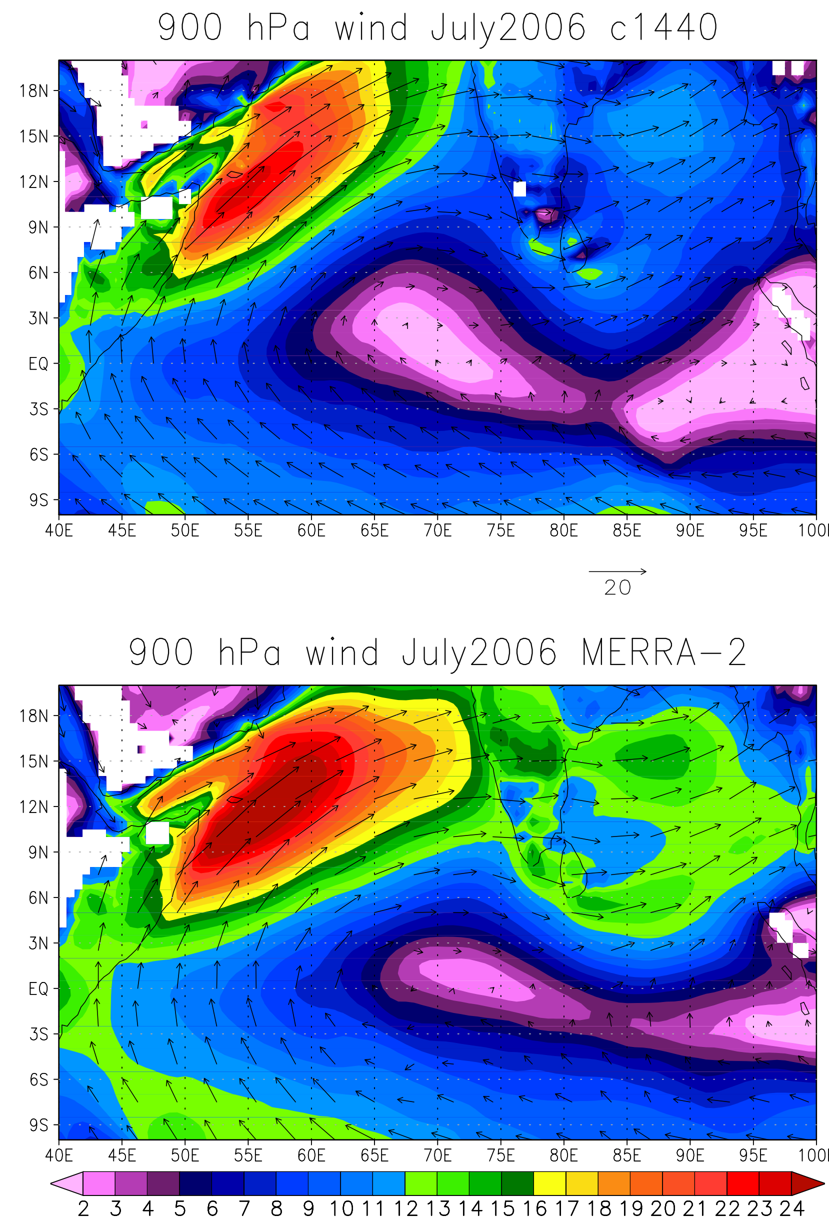

FIG. 16. Wind in July 2006 at 900 hPa across the Indian Ocean in the G5NR (above) and in MERRA-2 (below).

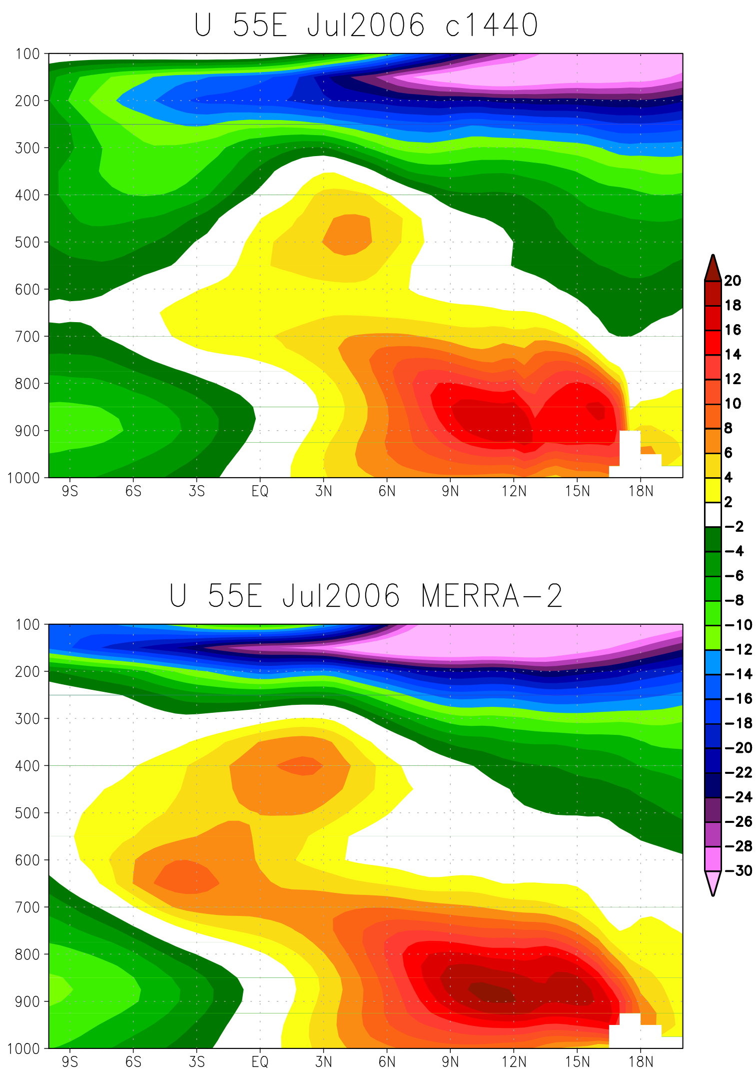

FIG. 17. Vertical meridional cross section of the Somali Jet in July 2006 and at longitude 55^oE in the G5NR (above) and in MERRA-2 (below).

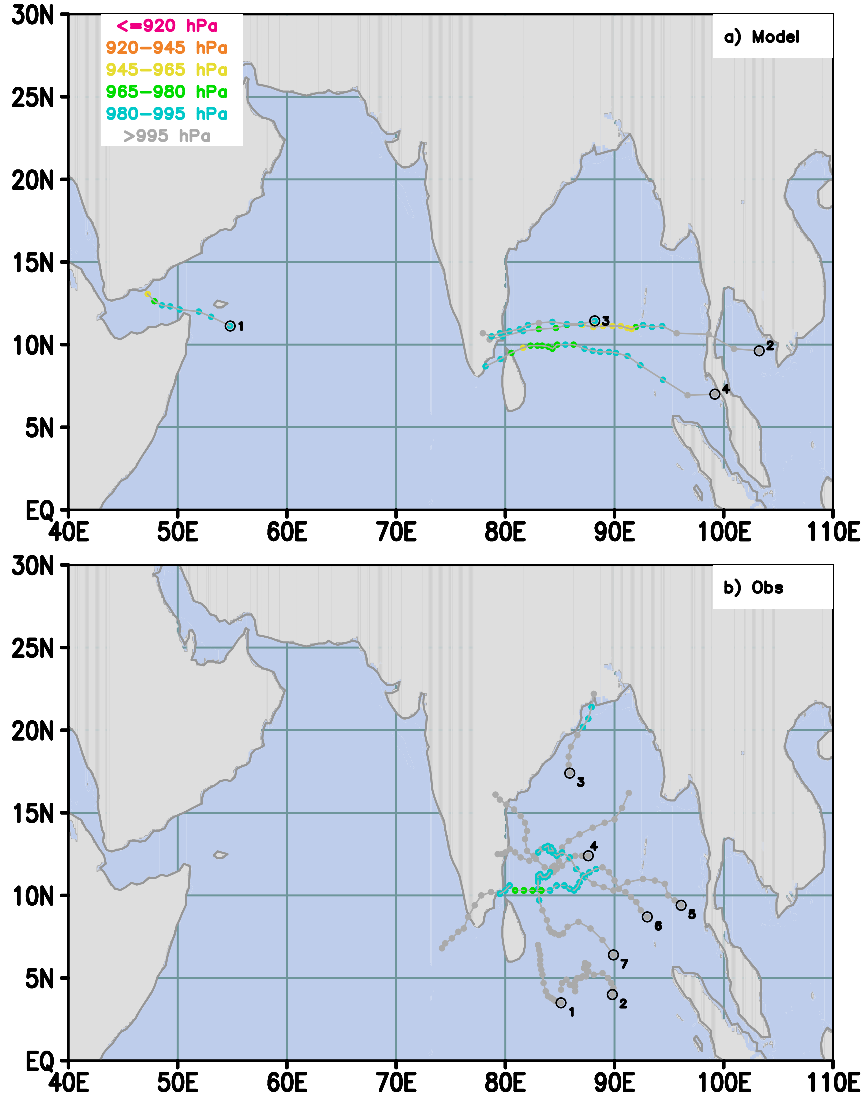

FIG. 18. Simulated and observed 2005 North Indian Ocean TCs from the G5NR (a) and BT (b). Colors as in Fig. 4. Corresponding dates in Table 7.

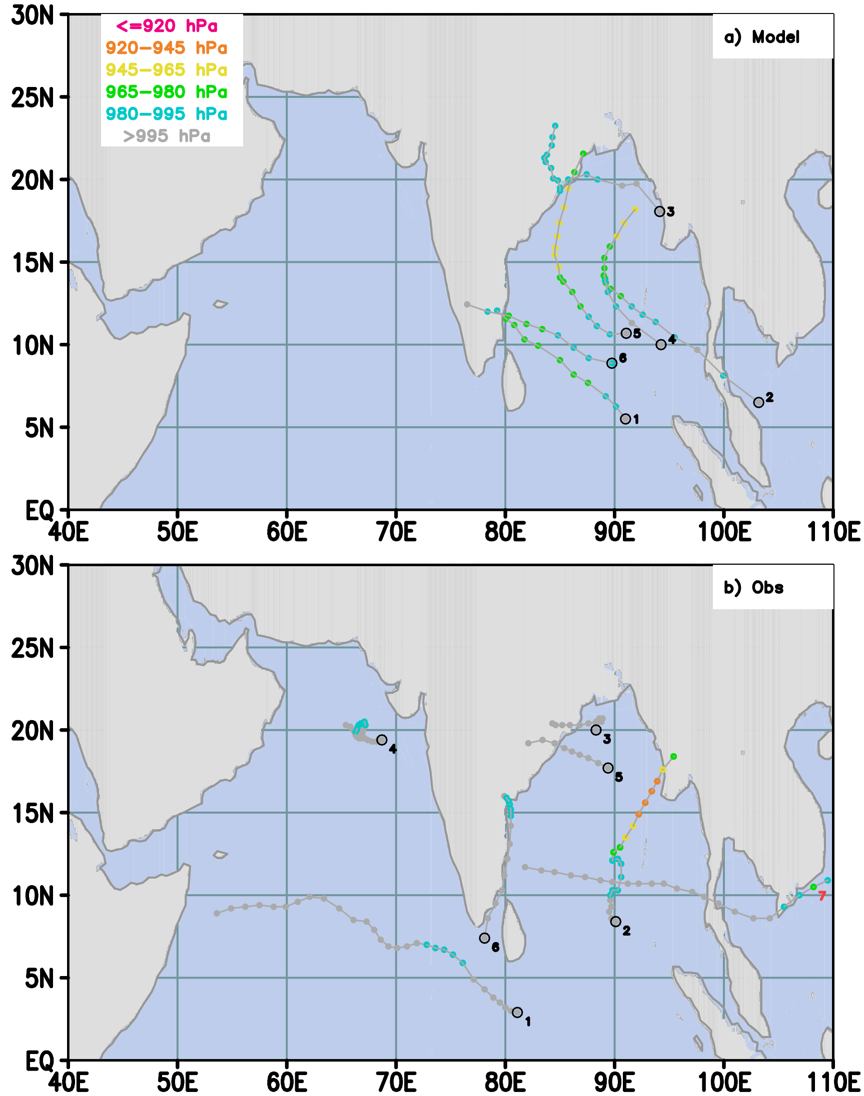

FIG. 19. Simulated and observed 2006 North Indian Ocean TCs from the G5NR (a) and BT (b). Colors as in Fig. 4. Corresponding dates in Table 7. Observed data show Typhoon Dorian (renamed TC 7) crossing the Malay peninunsula from the Pacific and entering the Bay of Bengal as a tropical depression

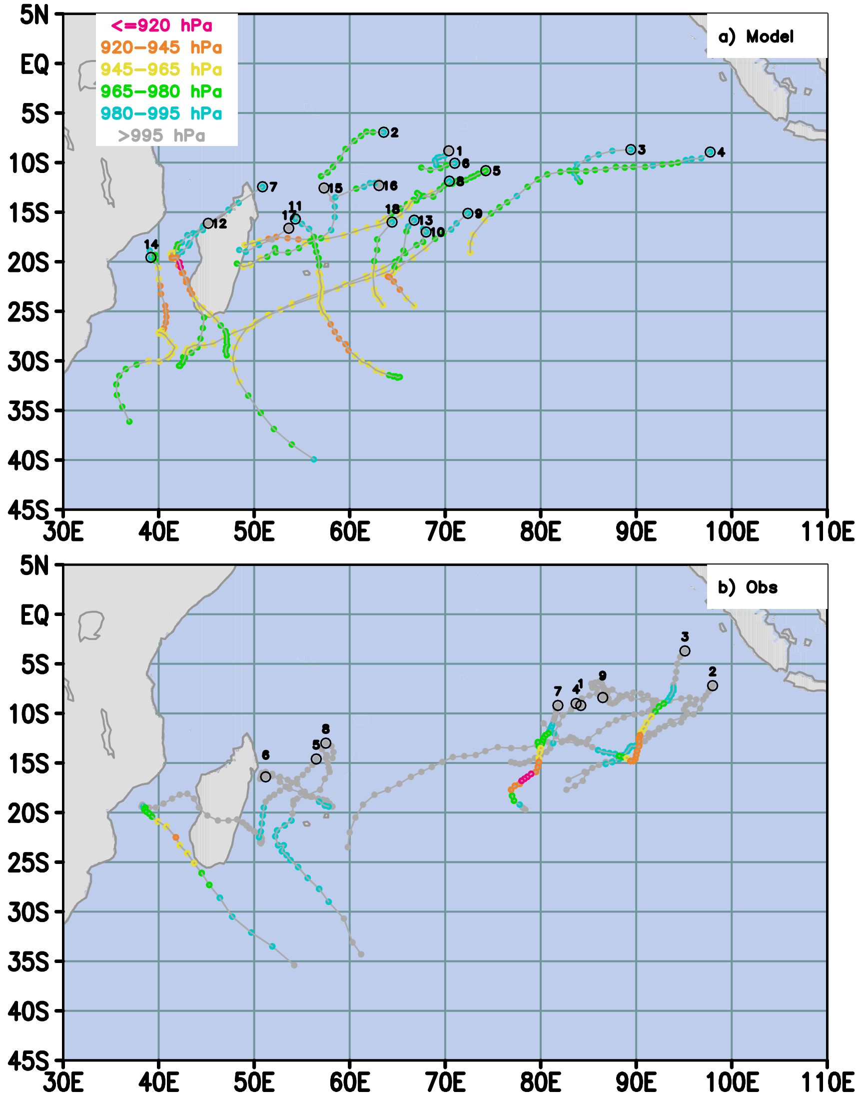

961 FIG. 20. Simulated and observed 2005-2006 South Indian Ocean TCs from the G5NR (a) and BT (b). Colors
962 as in Fig. 4. Corresponding dates in Table 8.

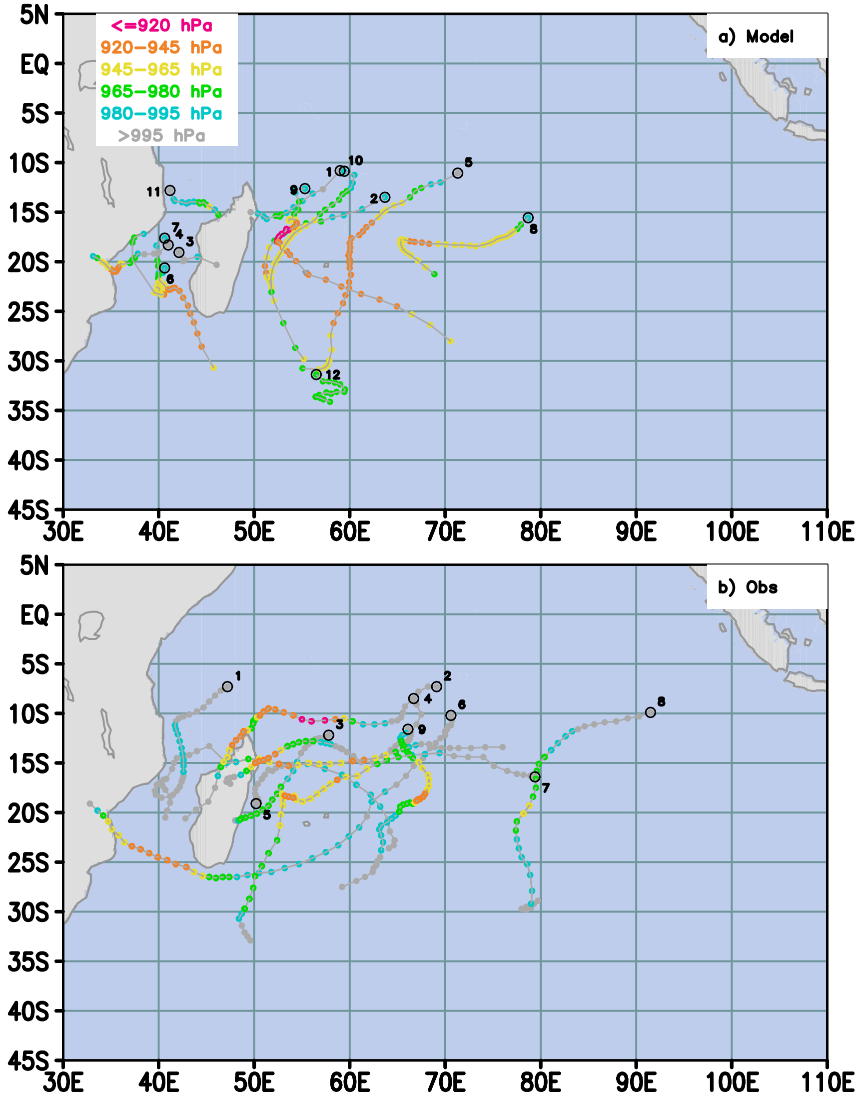

FIG. 21. Simulated and observed 2006-2007 South Indian Ocean TCs from the G5NR (a) and BT (b). Colors as in Fig. 4. Corresponding dates in Table 9.

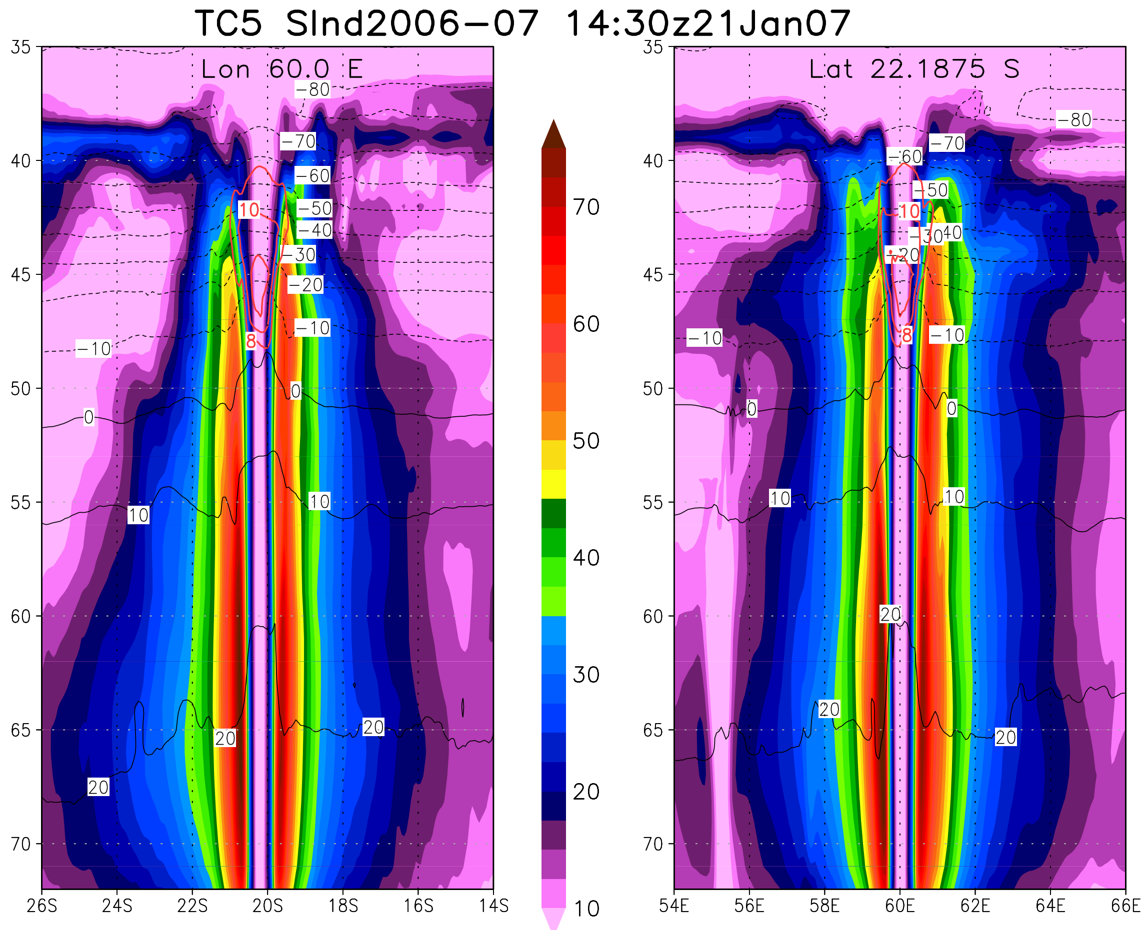

965 FIG. 22. Structure of G5NR 2006-2007 South Indian Ocean TC no. 5 (Fig 21 and Table 9). As in Fig. 6,
966 except that both zonal and meridional vertical cross-sections are plotted.

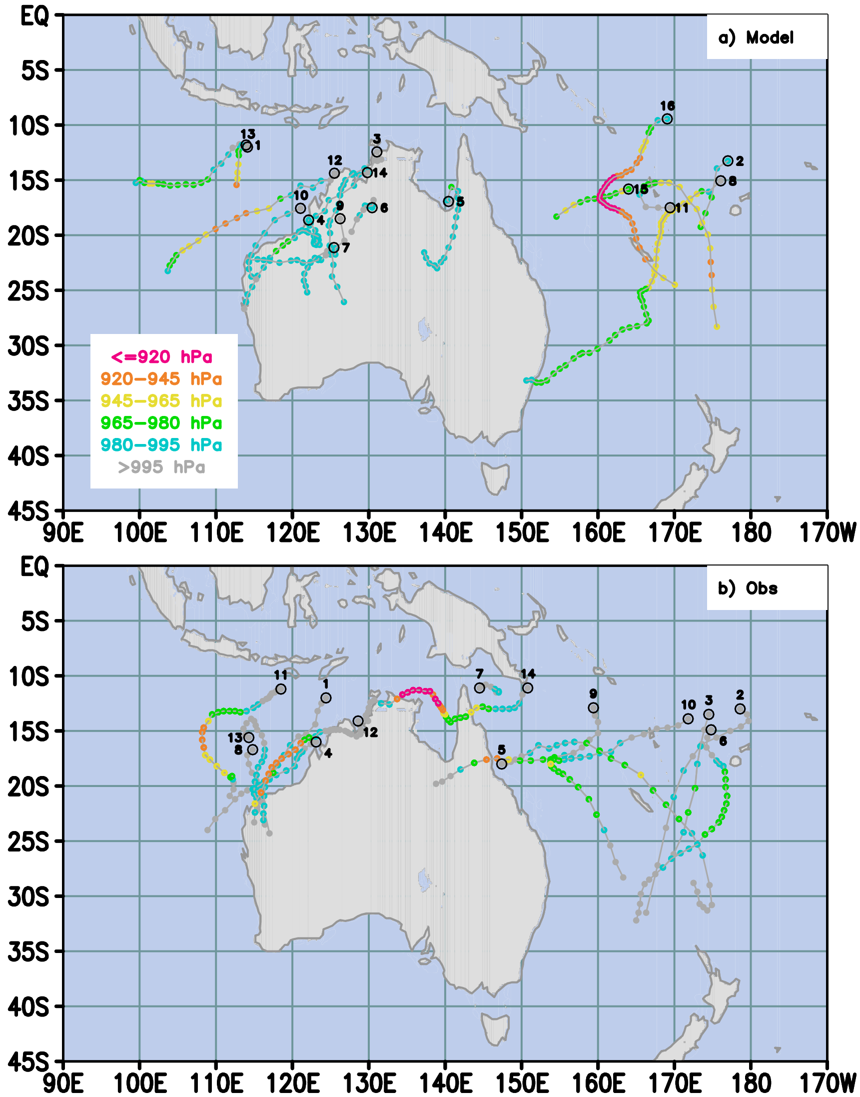

FIG. 23. Simulated and observed 2005-2006 Australian region TCs from the G5NR (a) and BT (b). Colors as in Fig. 4. Corresponding dates in Table 10.

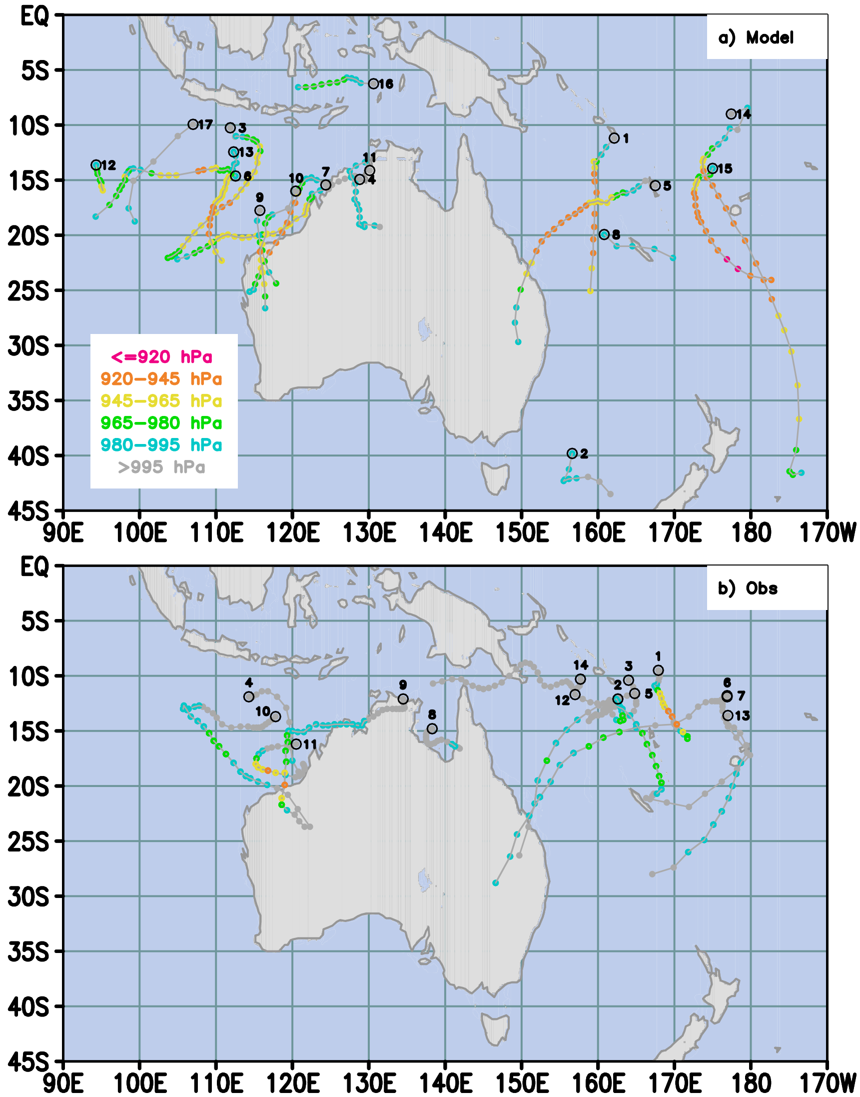

FIG. 24. Simulated and observed 2006-2007 Australian region TCs from the G5NR (a) and BT (b). Colors as in Fig. 4. Corresponding dates in Table 11.